

ME 450 – Design and Manufacturing III

Fall 2009

**Project 1: The Human Strider
Final Report**

Jie Hu

Spencer Slam

Brian Whitney

Section Instructor: Nikos Chronis

December 15, 2009

EXECUTIVE SUMMARY

The aim of this project is to design a device that will allow humans to move on the surface of water. Our target market is the recreational user, someone who will use the device as an enjoyable and unique mode of transportation.

The shoe, which will be close to the dimensions of a ten year old child's shoe, 20 cm long, 10 cm wide, and 10 cm tall, should be capable of supporting a person on the surface of a body of water. For our prototype, the shoe is designed for a child that weighs 40 kg (20kg per shoe). The shoe also needs to be stable and give the person the opportunity to move.

We generated twenty initial concepts. From our list of ideas five were selected as the most promising and were subjected to a more rigorous analysis and discussion. The five concepts were the wire leg shoe, the inflating balloon shoe, the thrust shoe, the hydrofoil shoe, and the vacuum shoe. We used a Pugh chart to quantitatively rate each of our designs against our specifications. We listed our most important requirements and specifications of our project and ranked them against each other to create our selection criteria. The hydrofoil shoe was determined to be the best concept.

After selecting the hydrofoil shoe as our alpha design, we revised the concept to use rotating hydrofoils instead of fixed hydrofoils propelled through the body of water. This concept allows the user to be stationary on the water's surface as well as to move, where the original concept required constant forward movement.

The rotating hydrofoil shoe design was rigorously analyzed to determine our final design. Our final design uses a DC motor powered by a battery pack and three hydrofoils that rotate at approximately three-hundred rotations per minute. The size and parameters of this shoe were determined using engineering analysis concerning lift, drag, power and strength of materials.

The prototype design differs slightly from the final design. The prototype shoe, which we built and tested, consists of only one of the two shoes needed for a person to properly use the device. It is also powered by a power supply instead of a battery pack. This is due to budget constraints. The prototype underwent a validation process which sought to quantify the produced lift and other important metrics.

The prototype did not perform as expected during validation. No measurable lift was generated during testing essentially failing to meet our most important criteria for success. Lack of lift generation could be due to a higher than expected drag, to vortices produced that caused a lower relative speed of the water to the hydrofoil and to other losses due to vibrations and instability. Through further testing and more rigorous fluid analysis this design can be improved and it can be determined whether it is a viable concept. If the concept does not prove viable we have laid forward a wide range of alternate concepts that can be pursued in the continuing effort to make a human water walking device.

Table of Contents

1. INTRODUCTION	5
2. LITERATURE REVIEW	5
Water Walking in Nature	5
Buoyant Water Walking Shoes.....	7
Hydrofoils.....	9
3. PROJECT REQUIREMENTS AND ENGINEERING SPECIFICATIONS	10
4. CONCEPT GENERATION.....	11
Wire Leg Shoe	11
Inflating Balloon Shoe	12
Thrust Shoe	13
Vacuum Shoe	14
Hydrofoil Shoe.....	15
5. CONCEPT SELECTION	15
Revised Concept Description	16
6. PARAMETER ANALYSIS.....	17
Airfoil Shape	17
Lift	18
Drag.....	19
Required Power.....	20
Strength Limitations of Connecting Rods.....	20
7. PROTOTYPE DESIGN DESCRIPTION	21
Electric Motor and Controller	22
Upper Housing	22
Gear Train.....	23
Rotor Assembly	23
8. FINAL DESIGN DESCRIPTION	24
Two shoes	25
Battery pack	25
Protective cage.....	25
Control system	25
Material choices.....	25
9. FABRICATION PLAN	26
Manufacturing.....	26
Top housing.....	26
Bottom housing.....	26
Hydrofoil hub	26
Hydrofoils.....	26
Keying Process	27

Adapter	27
Assembly	27
Top Sub-Assembly	27
Hydrofoil Sub-Assembly	30
Final Assembly.....	31
10. VALIDATION PROCEDURE AND RESULTS	32
Experimentation Plans Prior to Design Completion	32
Final Testing Procedure.....	33
Safety protocol for testing	35
Validation Results.....	35
11. DISCUSSION.....	38
Greater drag.....	38
Tip losses	38
Vortex effects.....	39
Container turbulence	40
12. RECCOMENDATIONS.....	40
13. CONCLUSION.....	40
APPENDIX A: Bill of Materials	41
APPENDIX B: Engineering Changes	43
APPENDIX C: Design Analysis Assignment	46
Material Selection - Functional Performance	46
Bottom Housing	46
Hydrofoil Shaft.....	46
Material Selection - Environmental Performance	47
Manufacturing Process Selection.....	52
APPENDIX D: Alternative Design Concepts	54
APPENDIX E: MATLAB Code for Power Optimization	58
APPENDIX F: Detailed Engineering Drawings.....	59
Appendix G: QFD.....	63

1. INTRODUCTION

We have undertaken the challenging task of designing a device that will allow humans to move on the surface of water. This project, sponsored by Professor Nikos Chronis, broadly aims to create some device that is close in size to a human footprint to allow such a feat. Our target market is the recreational user, someone who will use the device as an enjoyable and unique mode of transportation. Though attempts have been made by inventors previously, no satisfactory design has been created that allows a person to walk on the water's surface with ease and fluidity.

In our previous reports we detailed the initial findings on the topic, the customer specifications, and possible concepts that could achieve our goals. We ultimately settled on a design utilizing rotating hydrofoil blades to produce lift. We then proceeded to manufacture and test a prototype device.

2. LITERATURE REVIEW

A review of scholarly literature and patents provided background on several topic areas relevant in the design of water-walking shoes. Initially, we reviewed examples of water-walking behavior in nature in an effort to understand how such locomotion is achieved by various animals. This led to studies of hydrophobicity and how it can be used to amplify surface tension effects using modern materials. Finally, we reviewed existing designs for water-walking shoes, all of which use buoyancy to achieve flotation.

Water Walking in Nature

Though humans may be biologically limited to walking on terra firma, the animal kingdom can claim a variety of creatures capable of walking on the water's surface. Taking a biomimetic approach to design, the team has sought to understand the physics behind these animals' abilities. A large body of scholarly research from the biology world exists trying to understand this behavior[2].

The most familiar example of water surface locomotion is the water strider. The water strider insect, family *Gerridae*, is an insect often seen gliding across the surface of ponds, rivers and the ocean[1]. These arthropods, weighing in at a mere 1-10 dynes[2] are capable of supporting their weight *above* the water's surface. Being denser than water, buoyancy alone could not account for such a feat. Instead, the insects use surface tension to support their body weight[3]. Recently, research has suggested that this ability is largely related to the micro-structure of the insect's legs as opposed to their waxy coating as was previously believed. The study found that nano-scale grooves on the hairs covering the insect's legs contribute to their hydrophobicity and thus the strong surface tension achieved[4].

Surface tension is a phenomenon owing to the hydrogen bonds which attract water molecules to one another. The upward force exerted on an object is proportional to the perimeter of the object in contact with the water's surface. While the effect is capable of supporting small insects, larger animals cannot exploit the physics of surface tension.

It is possible to maximize the effective surface tension force at the interface by using hydrophobic or super-hydrophobic materials. Some examples of hydrophobic surfaces in the natural world are water strider legs and the surfaces of leaves which induce beading of water. Hydrophobic materials result in a

higher surface tension force due to a larger contact angle with water. For super-hydrophobic materials, this contact angle is over 150°[5]. The surface tension force exerted on a floating body normal to the flat surface of liquid can be calculated by following equation[6]:

$$F = \sigma L \cos \theta \quad (\text{Eq. 1})$$

Where F is the force exerted perpendicular to the liquid surface, L is the length that contacts the liquid surface, θ is the contact angle and σ is the surface tension of water. The contact angle is measured as the angle of the meniscus at the liquid-solid interface relative to the flat free surface of the liquid as shown in Figure 1 below:

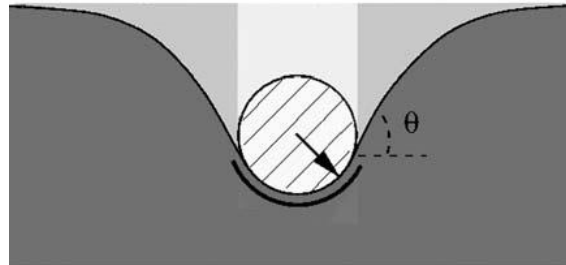


Figure 1: The contact angle of an object on liquid surface [3]

By increasing the contact angle using a non-wetting super-hydrophobic material, the surface tension force is effectively increased. Some of the recent improvements in super-hydrophobic materials involve nanofabrication and application to nonorganic material such as stainless steel (Figure 2)[7]. These materials could be exploited to maximize surface tension effects in a design that required surface tension force to support a large weight.

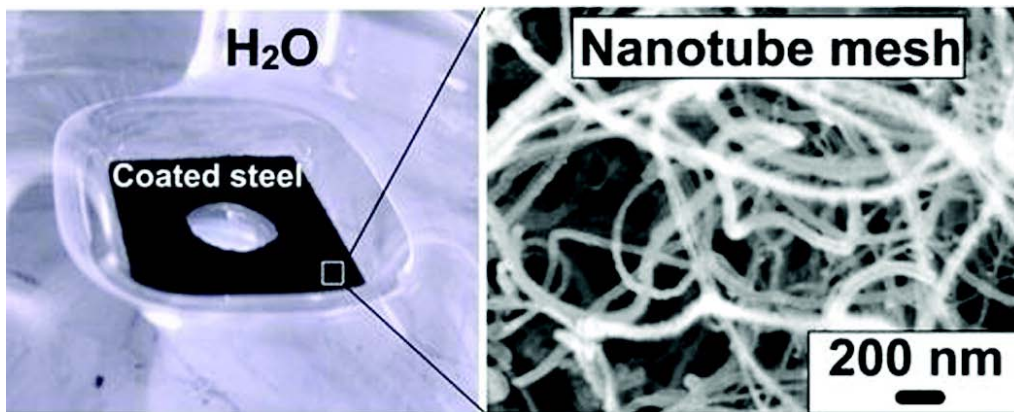


Figure 2: Super-hydrophobic conductive carbon nanotube coatings on steel [9]

A commonly used metric for determining the surface walking ability of an animal is the Baudoin number:

$$Ba = \frac{Mg}{\sigma P} \quad (\text{Eq. 2})$$

Where Mg is the weight of the creature, σ is the surface tension of water and P is the contact perimeter of the legs². A Baudoin number of $Ba < 1$ indicates a creature capable of resting on the water's surface¹. The natural form of a human being results in a Baudoin number far above one.

Aside from the Baudoin number, another physical constraint of the surface tension effect is apparent upon review of a 1998 paper by Joseph Keller which proves, as an extension of Archimedes' principal, that the upward force on a body partially submerged in water is equal to the weight of water displaced by the body and the surface tension meniscus combined^[8]. This would mean that a 70 kg human would have to displace 70 liters of water in order to support himself regardless of whether through surface tension effects or buoyancy. This truth may impose a limit on the scaling of surface tension effects which could prohibit its use by larger animals.

There are some animals with a Baudoin number of larger than one that are capable of water surface locomotion^[9]. Most notable is the Basilisk lizard which can run across the surface of the water with quick slapping motions of its feet at speeds of approximately 1.6 m/s but only for a short distance². A study of this behavior revealed that the lizard uses its pad-like feet to create a bubble of air in the water below it. The vertical component of the drag force achieved counterbalances the lizard's weight and the air cavity allows for the foot to be lifted at the end of each stroke^[9].

Buoyant Water Walking Shoes

Some previous work has been done by inventors in designing water walking shoes that use buoyancy to support a human. While our current size specifications do now allow for us to use buoyancy as a sole means of flotation, these patents give us insight on what work has been done in this area and allow us to learn from other people's struggles. The first patent worthy of discussion is titled "Apparatus for walking on water"^[10]. A picture of this patent is shown below.

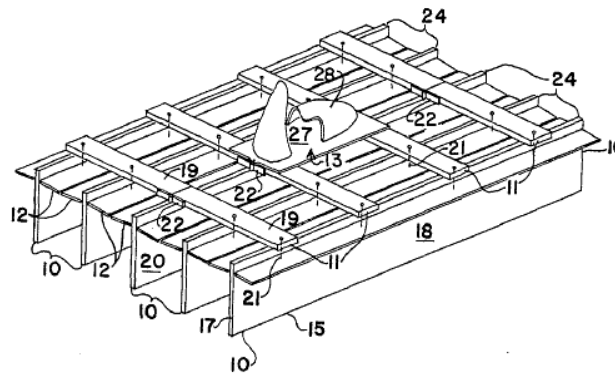


Figure 3: Ribbed Water Walking Shoe

This design has approximate dimensions of 100 cm long and 50 cm wide and uses buoyancy to float. These dimensions are about 5 times the length and width of our specifications. This apparatus is too bulky to carry around and would be hard to transport from one place to another. This device is made to be very stable and enable motion which is something that we will want to have in our final product.

Another design for shoes that walk on water is “Water walking shoes”[11]. The shoes in this design are bell shaped as shown below. Like the previous patent, these shoes use buoyancy as a means of floatation and are too large to be easily transported by hand.

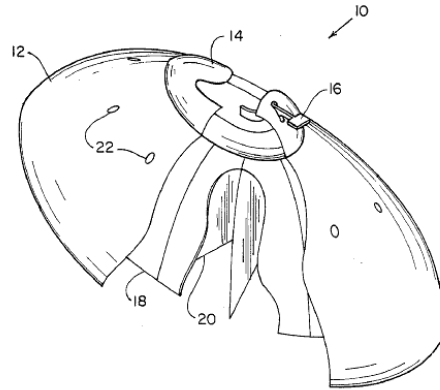


Figure 4: Shell Water Walking Shoe

These shoes are designed so that they overcome the suction effect experienced when lifting your feet. The shoes are easily picked up so that you can use a walking motion rather than a striding motion. Although these shoes allow you to walk on water, they are very bulky and would be difficult to travel with. The design would also prohibit using the shoes for walking on solid ground.

A third example of water walking shoes is found in the patent titled “Water Walkers”[12]. The shoes in this design are ski shaped shoes that are approximately 1.5 meters long. This design is shown in the figure below.

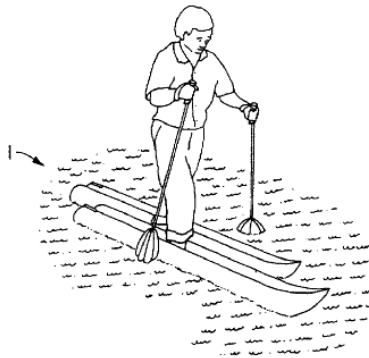


Figure 5: Canoe Water Walking Shoes

These shoes are very large and would be difficult to transport. In addition to that, the length of the shoes makes it very difficult to turn much like the difficulty experienced turning in skis on flat ground. For stability, the user of these shoes uses two poles to maintain balance[12]. These poles could be a valuable feature to help with stability for our own design.

Overall, the reviewed patents gave us insight about what has been done in the past and how to improve upon it in the future. After analyzing these patents we were able to create benchmarks and specifications that we intend to achieve with our design in order to improve upon previous concepts and create a new and innovative approach. We next looked to see if we could create something smaller that could generate lift and researched hydrofoils.

Hydrofoils

Hydrofoils were first used in watercraft design around 1900[13]. Since its introduction, the hydrofoil has been used extensively on high speed and small to medium-sized passenger boats due to its effect of lifting the boat out of the water. With less area contact with water, there is less resistance or drag [13].



Figure 6: Hydrofoil passenger boat KATRAN-3 [15]

Hydrofoils work in the same way as an airfoil; it is essentially the same thing operating in water instead of air. Lift force is determined using the following equation[14].

$$F_L = \frac{1}{2} \rho v^2 A_L C_L \quad (\text{Eq. 3})$$

Where F_L is lift force generated; ρ is the density of fluid the hydrofoil is passing through; v is velocity of the hydrofoil; A_L is planform area, which is the area observed from top of hydrofoil; and C_L is coefficient of lift, which is closely related to the shape of the hydrofoil. The main reason why hydrofoils can create more lift force than airfoils is the increase in density of fluid. Water has a density of 1000 kg/m^3 , which is approximately 1000 times that of air.

On the other hand, hydrofoils also have more drag force generated than airfoils due to the high density of water. The equation for drag is very similar to that of lift, as shown below [14].

$$F_D = \frac{1}{2} \rho v^2 A_D C_D \quad (\text{Eq. 4})$$

Where F_D is the drag force create by the water to push the user backward due to the motion forward; A_D is reference area, which is the area of the shoe projected perpendicular to the direction of motion; and

C_D is coefficient of drag. Due to its shape, the hydrofoil has low coefficient of drag and high coefficient of lift.

One of the restrictions on the use of commercial hydrofoil crafts, which have advantages in comparison with common displacement ships, is the necessity for specialized maintenance of the foil systems. Such work usually requires complicated equipment and experienced specialists[15]. After researching different types of ways to generate the force needed to stay on the surface of the water, we created our engineering specifications.

3. PROJECT REQUIREMENTS AND ENGINEERING SPECIFICATIONS

The broad goal of our project is to create a device, close to the normal dimensions of a normal walking shoe that will be capable of supporting a person on the surface of a body of water. For this initial foray into the world of surface locomotion our requirements for success are only to support the weight of a child on the surface of the water statically. An adult mass and the dynamic forces generated by walking both would increase the load-bearing requirement of the shoes. The target specifications for a close-to-average shoe size supporting a small child are listed in Table 1.

Table 1: List of specifications

Specification	Target Value
Shoe length	20 cm
Shoe width	10 cm
Shoe thickness	10 cm
Shoe weight	< 0.5 kg
Total supported load (in H2O)	40 kg
Able to turn	Yes
Stable during use	Yes
Easy to wear	Yes
Means of attaching to street shoe or foot	Yes
Reasonable use life	Yes
Safe for a human to wear	Yes
Overall cost	\$400

The average weight of an 11-year-old was determined to be approximately 40 kg[16] and the dimensions for the footprint were established from the project assignment summary. The target specifications were also incorporated into a Quality Function Deployment (QFD) chart to correlate them with the customer needs. The complete QFD can be found in Appendix G.

In order to evaluate our own targets and project goals it was necessary to consider other devices in the field and use them as a performance benchmark. As a normal-sized water walking shoe has never been created there is little in the way of a reasonable benchmark. There are no water walking shoes on the

market, however a number of patents have been issued for buoyancy-based solutions. Due to the Archimedes principal the requisite volume of these shoes is inconveniently large. Although the volume has been arranged differently for various designs it will always inhibit the ability to walk with a regular stride due to interference between the shoes and the weight required to be lifted for a normal step. The specifications of our own design, therefore, are targeted to overcome the disadvantages of the existing patents. From these specifications, we generated our initial concepts.

4. CONCEPT GENERATION

In the concept generation stage many ideas were generated using various schemes in order to support the required load. These ideas ranged from reasonable to completely impractical. All of the generated ideas were recorded and broadly categorized based on the physical mechanism used to support load, be it buoyancy, surface tension, dynamics effects or another effect. From the list of ideas, five were selected as the most promising concepts and were treated to a more rigorous analysis and discussion. Those five selected concepts are discussed below. A more extensive list of concepts considered along with sketches can be found in Appendix A.

Wire Leg Shoe

The wire leg shoe is a shoe that relies almost completely on surface tension to create the upward force needed to keep a person afloat on water. The concept behind this shoe is to mimic the way a water strider remains on the surface[17]. Surface tension is the attraction between a liquid's molecules due to intermolecular forces[18]. The equation for surface tension is given by Equation 1 above. The surface tension value of water is 0.0734 N/m at standard temperature and pressure[19]. The contact angle, θ , varies for different surfaces. For our calculations we approximate the contact angle to be close to 180° due to the possible use of super-hydrophobic materials[20]. Approximately 200 N of force is needed to support the 20 kg as listed in our specifications. Using the values stated above, approximately 2700 m of contact length would be needed to create the necessary force. For this design, we would use thin wires to create the contact length. Each wire would contact the water on both sides and require us to have a total length in wire of 1350 m. The equations to calculate the force needed neglect the effects of buoyancy because the density of the shoe would most likely be similar to the density of water. If the shoe was much less dense than water, a small buoyant force may occur that would lessen the amount of contact length needed to support 20 kg. A preliminary sketch of this design is shown below in Figure 6:

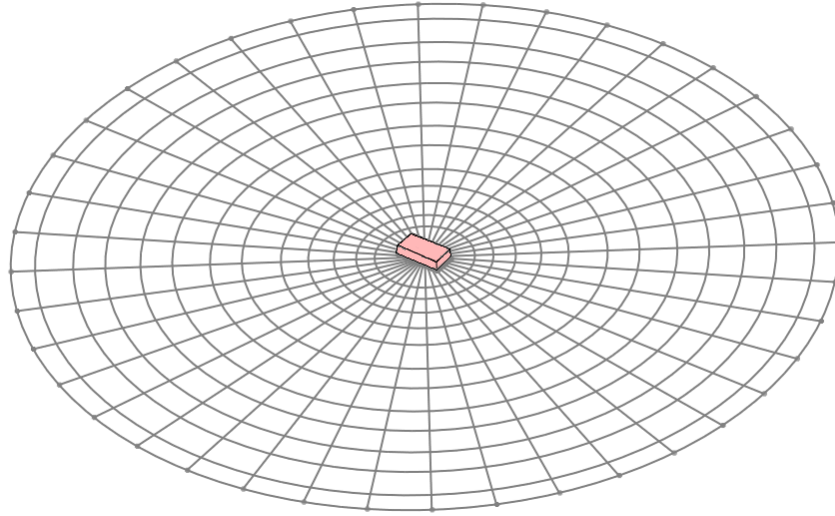


Figure 7: Wire Leg Shoe

While the above figure is not drawn exactly to scale, it was found that the radius of wire grid for such a design would be approximately two meters.

Inflating Balloon Shoe

The most intuitive way to create lift on water is through buoyancy. The equation to calculate buoyant force is as follows[21]:

$$F = mg - \rho Vg \quad (\text{Eq. 6})$$

Where F is the net force, m is mass of an object, g is gravitational acceleration, ρ is the density of the liquid, and V is the volume of the liquid displaced by the object. In order for an object to float, the ρVg term must be greater than the mg term. For this shoe, we want the net force to be zero so that the shoe will be stable. To determine the volume needed to be displaced the weight of the shoe and person system must first be determined. This weight is 40 kg (the weight of the person) plus any additional weight of the shoe. Assuming the shoe plus any additional apparatus weights 10kg, the total amount of displaced water need to be 50 liters as the density of water is 1kg/liter. If the shoe constructed was 50 liters in volume, it would not be an improvement upon current designs of buoyancy shoes and not meet our size specifications. The size of the shoe would need to be approximately 50cm long, 30 cm wide, and 35 cm thick. A preliminary sketch of this design is shown below in Figure 8:

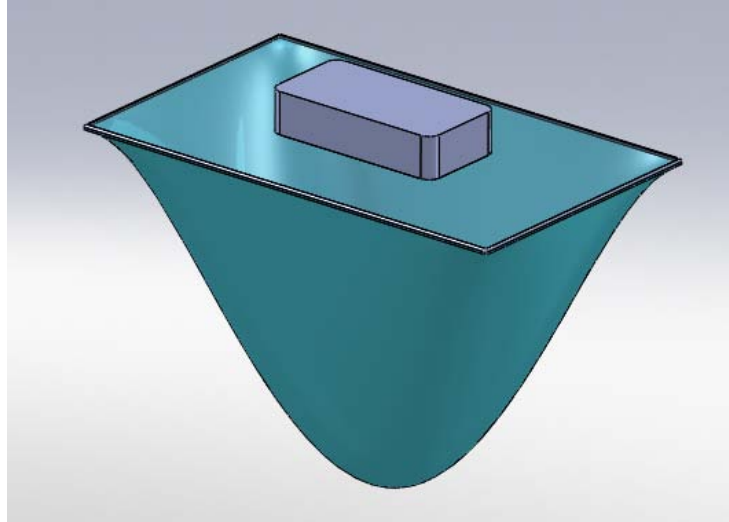


Figure 8: Inflating Balloon Shoe

What this design does different than previous buoyant shoes is that the shoe is not always the 50 liters in volume. This shoe will have a membrane attached to it that will inflate to 50 liters when the shoe enters the water and deflate when the shoe exits the water. This allows for the user to actually walk upon the water and is much more compact than current buoyant shoes.

For this design, the membrane should be able to inflate and deflate in 5 seconds or less. The reason for this is so the user can walk at a reasonable speed without having to wait a long time between steps. The volume flow rate of air needed to inflate and deflate the membrane is 10 liters per second. The way to achieve this would be with a vacuum pump and compressor.

Thrust Shoe

One possible design approach for balancing the walker's weight is the use of a vectored thrust. Thrust force is dependent on expelling mass in the direction opposite to the desired thrust vector. Through conservation of momentum, this expulsion generates a thrust dependant on the mass and velocity of the substance that is expelled. In this case the substance expelled could be water, air or some other fluid. Water and air are the most favorable due to their being readily available to the walker. Thrust is governed by the equation[22]:

$$F_T = \frac{dm}{dt} V = \rho V^2 A \quad (\text{Eq. 7})$$

Where F_T is the thrust force, dm/dt is the mass flow rate, V is the expelled fluid's velocity, ρ is the fluid density and A is the cross-sectional area of the exhaust nozzle. In order to support a weight of 200 N (~20 kg mass) a circular water jet 5 cm in diameter would need an exhaust velocity of approximately 10 m/s. To attain such an exhaust velocity would require a very powerful pump. Available pumps of such a power range weigh more than the walker. This realization makes such a system impractical for a water walking device as the total power output would need to be expended solely to support the device alone.

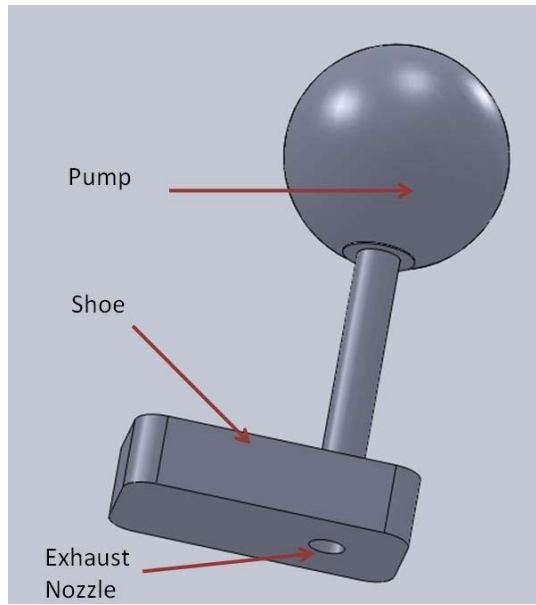


Figure 9: Thrust shoe schematic

Vacuum Shoe

Hydrostatic pressure in water is depth-dependant with increasing depth yielding a higher pressure which acts on any surface at that depth. It is the difference between pressures at different depths that is responsible for buoyancy. If one were able to get rid of the hydrostatic pressure acting at the upper surface, the force exerted on the lower surface could act to support a larger weight. It is this concept that the vacuum shoe is based upon.

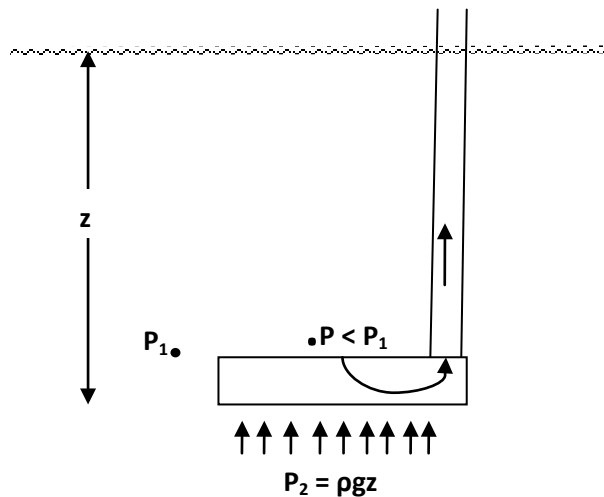


Figure 10: Vacuum Shoe Conceptual Schematic

By using a vacuum to lower the pressure on the upper surface of a block, a pressure difference could be created that is capable of supporting a load. Using our specified dimensions for the planar area of the

block, the surface would have to be at a depth of approximately one meter below the water's surface. This is based on the equation:

$$F = P_2A = \rho gz * A \quad (\text{Eq. 8})$$

Where z is the depth below the water surface and A is the area of the block. In order to create this effect some sort of pump must be employed. A major drawback of the vacuum shoe design is the necessity of extending the shoe to such a depth below the water's surface. Such an extension would seriously impeded movement and would not allow the user to walk in water of depth less than one meter.

Hydrofoil Shoe

The concept of using an airfoil through a moving liquid is employed in both aircraft and some watercraft. A hydrofoil generates lift by creating a pressure difference between the top and bottom of the hydrofoil. The top has less pressure than the bottom, so there is a net upward force[23]. If the upward force created by the hydrofoil is equal to the force due to weight, the total vertical force will be zero and it will be vertically stable.

The equation for lift is given in Equation 3 on Page 8.

In practice, some boats stack hydrofoils to create more surface area and more lift. This is the same principles biplanes use[24]. Using this same principle of stacking hydrofoils, it is possible to increase our lift and decrease our overall speed to a more reasonable level.

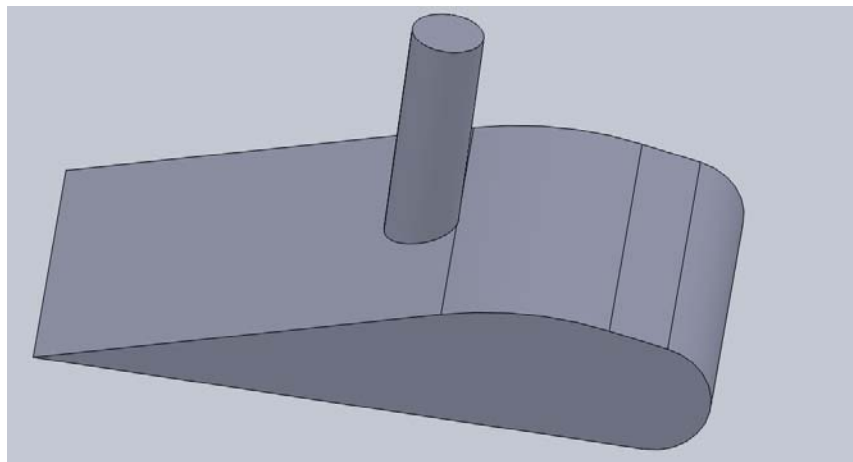


Figure 11: Hydrofoil Shoe

After generating the concepts, we proceeded to see which concept would best meet our specifications and scope of the project.

5. CONCEPT SELECTION

Rigorous analysis was done for each of our top five designs generated to determine which would be the best design. We used a Pugh chart to quantitatively rate each of our designs against our specifications.

To create the Pugh chart, we listed our most important requirements and specifications of our project and ranked them against each other to create our selection criteria.

The most important selection criteria for our project are the following: (1) the specified weight is able to be supported, (2) the dimensions in the specifications are met, (3) the design is safe, (4) movement is easy, and (5) manufacturing is feasible. According to our Pugh chart, the best design is the hydrofoil shoe with the inflating balloon shoe coming in second.

The wire leg shoe was disqualified because it greatly exceeded our maximum dimensions. The thrust shoe was disqualified because of the amount of thrust needed to keep the shoe afloat. The size of the device would generating the thrust would need to be very large and would introduce even more weight. The design was also deemed as relatively unsafe. The vacuum shoe was disqualified due to the feasibility of being able to create a design that could support the specified weight within the specified dimensions.

Since both the hydrofoil shoe and the inflating balloon shoe designs were relatively closely rated, further examination was done to determine which design would be the best choice. Preliminary manufacturing research and cost analysis was done to determine which project was more feasible. When looking at compressors for the inflating balloon shoe, one could not be found that could produce the volume flow rate needed to inflate the balloon quickly enough yet be small in size. These compressors were also very expensive. When searching for motors for the hydrofoil shoe, many types of motors were found that could generate the required thrust while still being small in size. The motors were affordable with our budget constraints. The hydrofoil shoe, number one from the Pugh chart, design was confirmed as our alpha design.

Revised Concept Description

After initially choosing the stacked hydrofoil concept for our alpha design, we have revised our design to a different manifestation of the hydrofoil lift principle. The decision to revise came from a design suggestion of a classmate and a reevaluation of the requirements of our original design.

The newly selected concept still uses the same principles of operation of a hydrofoil to create lift. The difference is in how the velocity of fluid over the foil is achieved. As opposed to moving the whole device and operator along the water surface, the revised design moves the hydrofoil blades themselves. The blades are rotated around a central axis and thus create lift without requiring a net motion of the user.

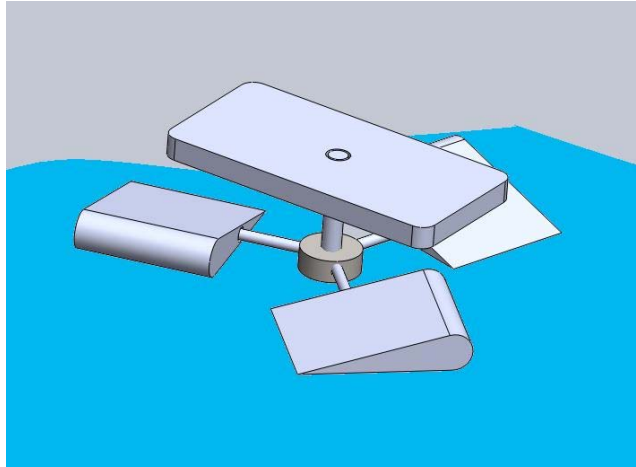


Figure 12: Rotating Hydrofoil Concept Model

The rotating hydrofoil design presents several distinct advantages over the initial stacked hydrofoil design. In the initial design the fixed hydrofoils were required to be constantly in motion relative to the water in order to generate lift. This condition puts significant practical limitations on the device. Firstly, the user is prohibited from standing still in one spot which is both inconvenient and unsafe due to difficulties in approaching the shoreline or other hazardous objects. The ability to create lift in a stationary position also gives the rotating hydrofoil the advantage being testable in any enclosed water body whereas the stacked foil design requires some sort of water tunnel with consistent flow.

Calculations confirmed that the power required to generate lift with the rotating hydrofoil was a reasonable value to expect from an appropriately sized motor. The calculations showed that the power required for the rotating hydrofoil was less than that of the stacked hydrofoil design. Whereas the stacked hydrofoil design requires converting electrical power to thrust in the propeller before generating lift in the wings, the rotating hydrofoil more directly produces lift and thus requires less power input. We then performed rigorous analysis to determine the exact parameters of these shoes.

6. PARAMETER ANALYSIS

Once the rotating hydrofoil design was selected, various engineering parameters were analyzed in order to determine the form that the device would have to take in order to meet our specifications. We first determined the optimal airfoil shape for our application. Once this was selected we were able to determine the conditions necessary to create the required lift. The corresponding drag and power requirements were then evident. All of this information, combined with strength requirements led to the implementation of our final design.

Airfoil Shape

The first parameter that was necessary to fix in order to analyze our device was the choice of airfoil, and the corresponding lift coefficient. We chose a standard airfoil shape that best corresponded to the particular needs of our device.

The shape of the hydrofoil we picked for our device is a National Advisory Committee for Aeronautics (NACA) 5-digit standard shape: NACA 23012 airfoil. There are several reasons for the choice of this particular shape. Firstly, 5-digit standard shapes have higher lift coefficients than 4-digit and 16-series, the other two standard shapes. Secondly, 5-digit airfoils are optimized for lower speeds than 6, 7, and 8-series, which is what we needed for our device. After some research into the specifications of 5-digit airfoil shapes, we decided to use NACA 23012 airfoil. The main reason is that this airfoil has a relatively high lift with a relatively low cost of drag. The first digit within the name '2', when multiplied by 3/2, yields the design's lift coefficient in tenths, 0.3. The next two digits '30', when divided by 2, give the position of the maximum camber in tenths of chord, 15% back from the leading edge. The final two digits '12' indicate the maximum thickness in percentage of chord, 12%[25].

Although the NACA database is based on performance of airfoils in air, a valid comparison can be made to operation in water. As a dimensionless unit, the Reynolds number characterizes the flow conditions of a fluid in such a way that it can be compared to any other fluid. By computing the Reynolds number for the hydrofoil ($\approx 500,000$) with the viscosity and density of water, we can find the equivalent velocity in air for the same Reynolds number. Through this process we determined the equivalent airspeed and thus optimal airfoil shape for our design. The Reynolds number equation is as follows[26]:

$$Re = \frac{\rho VL}{\mu} \text{ (Eq. 9)}$$

Where Re is the Reynolds number, ρ is density of the fluid, V is the velocity of the fluid, and L is the characteristic length.

Lift

The most fundamental specification that was used to guide our engineering analysis of the design was the required lift. Using our specified supported load of 20 kg, we were able to determine rotational velocities and torque requirements for various blade configurations. The equation for lift produced by a hydrofoil rotating around its endpoint was determined by integrating lift as a function of radius:

$$\begin{aligned} F_L &= \int_{r_1}^{r_2} \frac{1}{2} \rho C_L (\omega r)^2 l dr \\ &= \frac{1}{6} \rho \omega^2 l C_L (r_2^3 - r_1^3) \text{ (Eq. 10)} \end{aligned}$$

Where ρ is density of water, ω is angular velocity of the rotor, C_L is the coefficient of lift, l is the blade length and r_2 and r_1 are the outer and inner radii of the blade respectively. The calculated lift force is the lift produced *per wing* and thus the total lift produced will be equal to $n * F_L$ where the apparatus consists of n hydrofoils. The simple multiplication of the lift by the number of wings is an approximation. In reality the wings will induce a velocity in the water and thus the relative velocity of the water passing over the hydrofoil will be lessened. Such a configuration can only be accurately analyzed by using three-dimensional computational fluid dynamics software that is beyond the scope of this project.

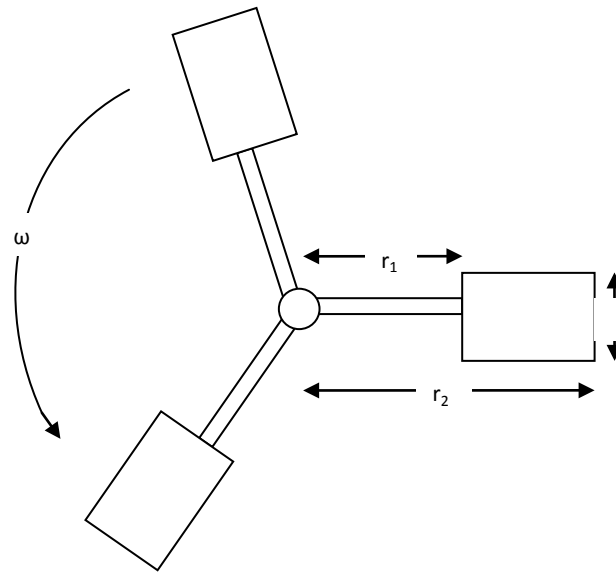


Figure 13: Definition of rotor dimensions

Drag

The next factor to consider is drag produced by the blades spinning through the water. As the drag acts along the length of the blade it will produce a net torque acting about the vertical axis of the rotor. The drag torque can be determined in a similar fashion to the lift, by integrating over the length. As the torque is also determined by the moment arm length, r , the drag produced is proportional to the difference of the fourth powers of r_2 and r_1 :

$$\begin{aligned}
 T_D &= \int_{r_1}^{r_2} \frac{1}{2} \rho C_D (\omega r)^2 r * t \, dr \\
 &= \frac{1}{8} \rho \omega^2 t C_D (r_2^4 - r_1^4) \quad (\text{Eq. 11})
 \end{aligned}$$

Where C_D is the coefficient of drag and t is the hydrofoil thickness. Again this torque corresponds to that of one blade. While drag, in general, is a function of Reynolds number, within the flow regime in which our device operates (approximately $Re=500,000$) the curve is fairly flat as shown in Figure 14. This allowed us to take an upper-end estimate of C_D and hold it constant.

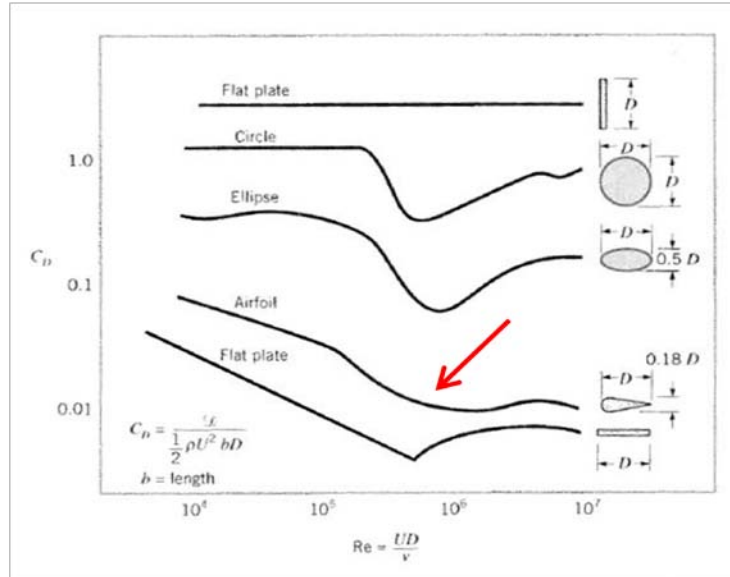


Figure 14: Coefficient of drag versus Reynolds

Required Power

Once the relationships between lift, drag and rotational velocity are understood it is possible to calculate the total power required to spin the rotors. This is a product of drag torque and rotational velocity[27]:

$$Power = T_D * \omega \text{ (Eq. 12)}$$

Using Equations 10 through 12, we created a MATLAB program that allowed us to explore various configurations of the rotor. The complete MATLAB code can be found in Appendix E. In this program we primarily focused on varying the number of hydrofoil wings and adjusting the wing size parameters accordingly to avoid overlaps while holding lift constant at the required 196 N. Through an iterative process we were able to establish that the required power is proportional to the number of rotor blades:

$$Power \propto n \text{ (Eq. 13)}$$

Thus, for a given lift the requisite power can be minimized by using the fewest number of blades acceptable

Strength Limitations of Connecting Rods

After consideration of power we next turned our attention to the practical limitations of different blade configurations. Use of a single blade can be eliminated as a possibility due to the inherent instability of such a configuration. We must consider the strength of the blade and supporting members. With two blades, half of the operating load would be supported by each, with three a third of the load would be supported, etc. Thus it was necessary to determine the minimum number of blades required to support the specified load of 20 kg. The point of failure will be yielding on the supporting rod where it connects to the central hub. Equations 14 and 15 below were used to calculate the maximum stress[28]:

$$\sigma = \frac{My}{I}, I = \frac{\pi}{4}r^4 \text{ (Eq. 14, 15)}$$

Where σ is bending stress, y is the distance to the neutral axis, and I is the area moment of inertia. The listed equation for I , with r been the radius, is used for circular cross section which apply to our application. The calculation indicated that two supporting members would *not* have sufficient strength to support our load based on the yield strength of steel and given dimensions. Due to drag limitations and the thickness of hydrofoils blades, the dimension of the connecting rods could not be altered. Thus, three blades, with three connecting rods, is the minimum requirement to support the required load. This gives us factor of safety of approximately 1.5.

Based on power, strength and drag considerations we found that the optimal number hydrofoil blades for our configuration is three.

Through our parameter analysis process we were able to establish the expected operating conditions of our device, as governed by our lift requirement, motor specifications and rotor design. The expected values are listed in Table 2 below.

Table 2: Target parameter values

Parameter	Target Value
Generated Lift	196 N (20 kg)
Angular Velocity	326 RPM
Steady-State Drag	0.753 N-m
Power	35 Watts

Some evaluations of material and manufacturing processes and environmental sustainability were performed use CES and SimaPro. PVC and stainless steel were two of the main materials used in our device due to water/rust resistance and availability. For manufacturing process selection, it was determined that thermoplastic injection molding and CNC lathe/turning should be the main process to mass manufacture given device according to CES. For environmental concerns, it was determined that cooling water usage and carbon dioxide emission are two main concerns according to SimaPro. The detailed analysis of material selection, manufacturing process selection, and environmental analysis can be found in Appendix C.

7. PROTOTYPE DESIGN DESCRIPTION

After completing our engineering analysis the calculated parameters were incorporated into a complete design. The design will consist of an electric motor, a sealed body containing the gear train and a rotor assembly consisting of three hydrofoils connected to a sing output shaft.

Electric Motor and Controller

A 24 V DC motor was selected as the power source for the unit. The motor was chosen for its power output and small size. The necessary power calculated from the parameter analysis is approximately 35 Watts.

Another power option that was considered was a gasoline two-stroke engine. The main drawback of a gas engine is the complication involved in using it in water. Gas engines require air intake in order to complete their combustion cycles. If the engine is submerged, the engine will stall and may suffer permanent damage[29].

A DC motor was chosen so that the motor could ultimately be powered by a battery pack. Although for the prototype the motor will be connected to a power supply which converts AC mains voltage into a 24 V DC signal, the motor is capable of being powered by a battery of sufficient power.

In addition to the motor itself a motor controller is necessary in order to control the motor's speed. The motor controller is connected directly to the DC power supply and to a potentiometer which is used to vary the output speed. In addition to providing a control system to the user, the motor controller acts as a failsafe device, not allowing current to exceed a threshold above which the motor could be damaged[30].

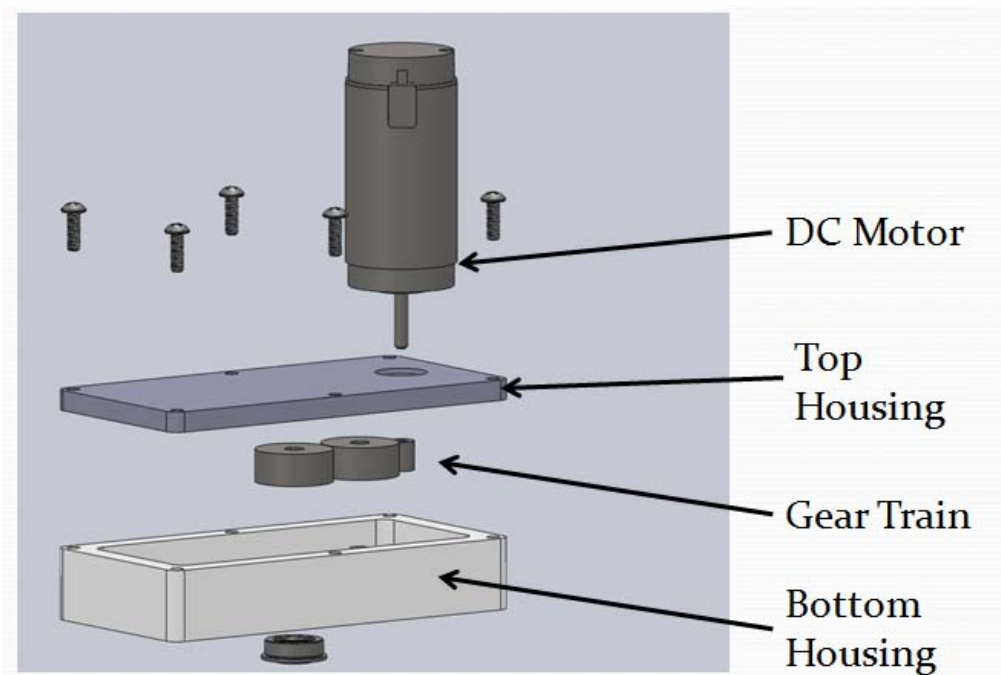


Figure 15: Exploded Gear Box Assembly View

Upper Housing

The upper housing is a PVC body which will be the main supporting structure on which the user will place his/her foot. The housing also contains the gear train and connects the motor to the rotor

assembly below. PVC was chosen as the building material for the housing due to its machinability, low weight, and availability at required stock sizes.

As the upper housing is the structure on which the user will place his/her foot, some means of attaching to the foot is necessary. Two simple nylon straps will provide a means of attaching the shoe. Nylon was chosen because of its high strength and low cost.

Gear Train

The gear train, located within the upper housing, transmits power from the motor to the output shaft while providing a 3:1 speed reduction.

The 3:1 gear ratio was chosen to place our targeted angular velocity in the middle of the torque/speed curve of the motor. As DC motors are optimized to operate in a high RPM, low torque regime a geared transmission is necessary to be able to operate at the torque range required for high torque applications such as our own[31]. The gearing is achieved through three spur gears, the last of which is connected to the output shaft and the rotor.

Rotor Assembly

The rotor assembly is the lift producing segment of the shoe. Via the transmission gears, power is transmitted to the rotating hydrofoils. The hydrofoils will create lift which is transmitted through the rotor structure and into the upper housing. The hydrofoils were placed at the maximum depth below the housing allowable according to our design specification of a total depth not exceeding 10 cm. The maximum depth was chosen to avoid possible interference and losses associated with the hydrofoil blades approaching the air-water interface.

Each hydrofoil is mounted on a steel rod which is connected to a central hub at the end of the output shaft. The hydrofoil dimensions are based upon the calculations from MATLAB analysis discussed previously and upon the tooling limitations of the CNC mill which cannot mill pieces much deeper than our 6 cm width.

The steel connecting rods will contribute drag torque during operation; however the torque will be lesser in magnitude than that at the tips due to a shorter moment arm. It was necessary to utilize a steel connecting rod rather than a continuous hydrofoil due to both strength and machining requirements.

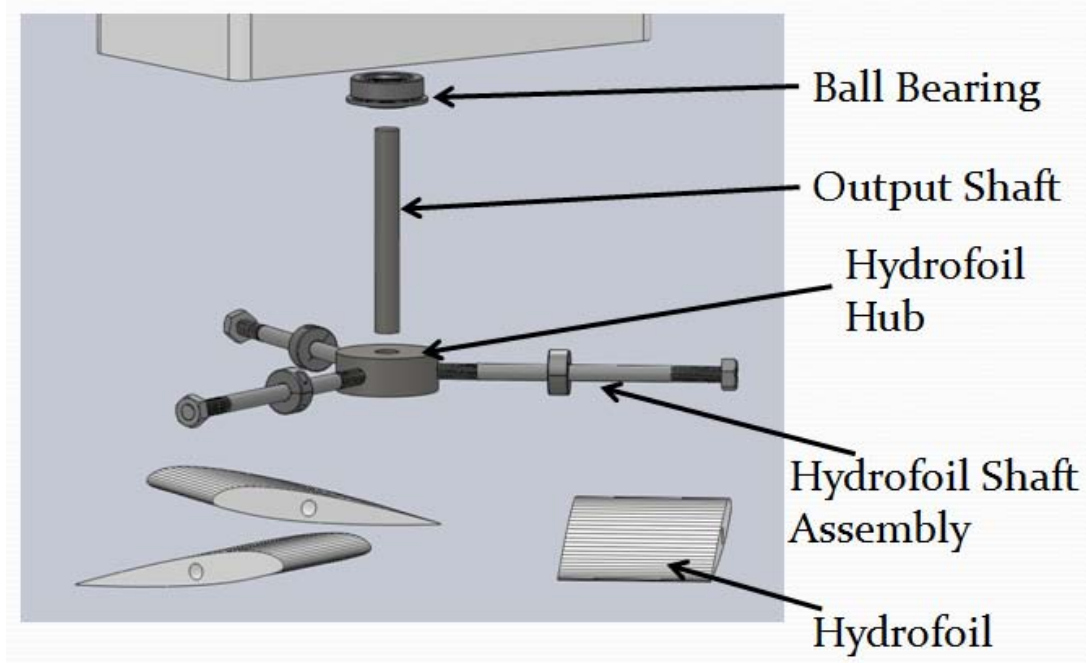


Figure 16: Exploded Rotor Assembly View

A more in depth discussion of each component is available in the fabrication plan below.

8. FINAL DESIGN DESCRIPTION

The final design, as shown below in Figure 17, is identical to the prototype design with the exception that there are two shoes instead of one and that there are more safety features. Anything not discussed in the section is to be assumed to be identical to corresponding part in the prototype.

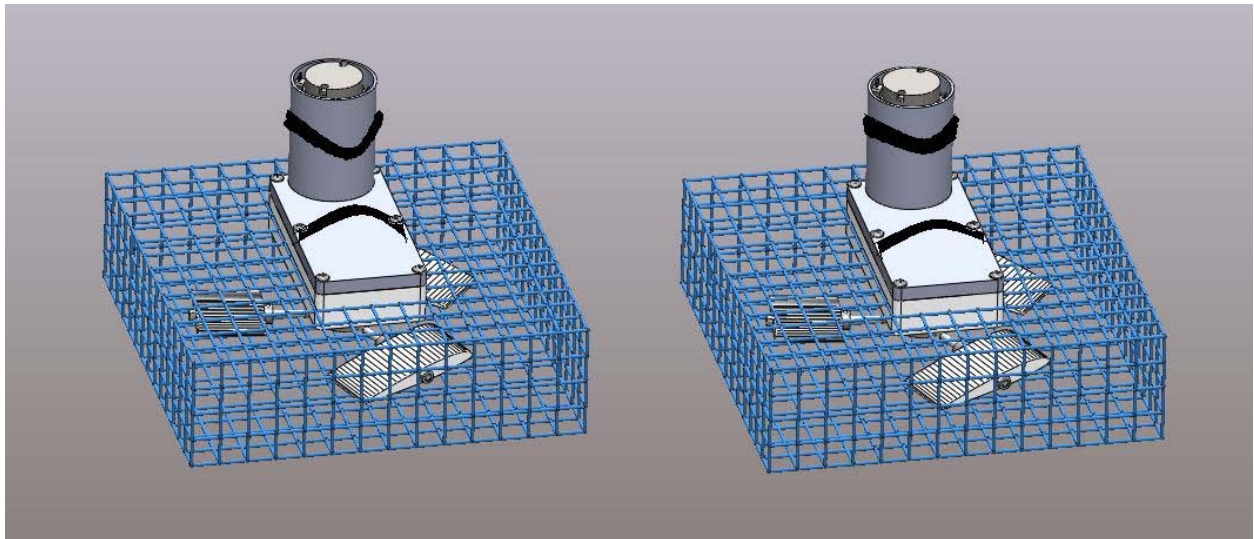


Figure 17: Final Design

Two shoes

The major difference between the prototype and the actual design is that only one shoe will be prototyped. The reason for this is mainly budgetary constraint, however time constraints are also limiting. Most of the budget has been consumed with the manufacture of one shoe, so it is not feasible to make two. The testing, as described in our validation approach, requires only one shoe.

Battery pack

The final design will use a battery pack as the source for power instead of a DC power supply so that the shoe is more mobile and can be used away from an electrical outlet. With the budget constraints of the project, a \$269 battery pack was not economically feasible for the prototype.

The battery pack used is a LiFePO₄ battery pack [32] that can supply the 24V and 3A needed power for each shoe. The battery weighs 3.7 kg and has a capacity of 15 amp hours. The battery pack is able to be split to power both shoes at the same time and can run for 2.5 hours before the need to recharge. It is also small enough to wear on a waist pack without much discomfort. The user will have a dial on his waist pack to control the speed of the spinning hydrofoils so that people of slightly different weights can all use the shoe. The extra weight of the batteries was taken into account for our specified speeds needed to lift the 20 kg per shoe.

Protective cage

There will be a protective cage around the hydrofoil shoes in the final design to prevent users from touching the spinning hydrofoils and to prevent the blades from damage. This cage will be rigidly attached to the bottom housing and have small enough holes so that the average appendage cannot penetrate it. Another added benefit of the cage is that it allows a person to equip the shoes on land and actually walk on land to get to the water. This would not be possible with the prototype because the blades would be damaged. Computational fluid modeling should be conducted to ensure that interference from the cage does not significantly impact the lift produced by the hydrofoils.

Control system

In order to address stability issues, a feedback control system could be implemented using MEMS gyroscopes and accelerometers as input sensors. By measuring the inclination and acceleration of each shoe independently the control system could determine whether the user is listing one way or the other and make the appropriate change in power input to each rotor to regain stability.

Material choices

In order to reduce weight in the final design, more lightweight materials can be utilized. Specifically, carbon fiber could be used for the hydrofoils. Titanium could be used for the gear train and connecting rods. Both of these material selections reduce weight while improving strength; their cost would certainly be a limiting factor. An additional benefit of lighter components is decreased inertia to overcome in the startup of the rotor.

9. FABRICATION PLAN

The fabrication plan is limited to the tools available in the machine shop. We manufactured four major components of our prototype. The other components were purchased. The following is a detailed description of how to manufacture and assemble the hydrofoil shoe prototype.

Manufacturing

The following manufacturing processes are used: CNC milling, manual milling, cutting, drilling, tapping, and press fitting. The risk of using these machines can be reduced by using the proper safety equipment, previous machining experience, and supervision when necessary. All extremely difficult or dangerous parts were purchased.

Top housing

The top housing of the device, as shown in Figure 1 above, is made out of 0.5"×12"×12" thick acrylic sheet for observation reasons. The acrylic sheet is cut to size using a laser cutter. Six holes are drilled by the laser cutter for attachment with the bottom housing using screws. There are four additional holes drilled by laser cutter for attachment with DC motor. There is also one larger hole drilled by laser cutter for shaft of the motor to go through. All machining dimensions are determined according to engineering drawings of the part.

Bottom housing

The case for gear and motor assemblies, as shown in Figure 2 above, is made out of 1.5"×12"×12" thick PVC that will be provided by Bob. The PVC should be cut to rough size using a band saw. Then, the PVC block is milled with a 3/8" mill bit at a cutting speed of 8000 rpm to make room for gears. There are six holes drilled on top of the box by drill press with a 1/4" drill bit at a cutting speed of 12000 rpm, and later taped with for attachment with top housing using screws. There is one larger hole drilled by drill press with a 1 1/8" drill bit at a cutting speed of 3000 rpm through the box for output shaft. All machining dimensions are determined according to engineering drawings of the part.

Hydrofoil hub

The connection hub between power transmitting shaft and hydrofoils, as shown in Figure 3 above, is made out of 1.5" diameter × 5/8" length steel rod. It is a purchased part. One hole is drilled by a drill press with a 1 1/8" drill bit at a cutting speed of 1500 rpm on one face of the hub. The hole is then be taped for attachment with threaded end of output shaft. Three additional holes are drilled by drill press with a 1/4" drill bit at a cutting speed of 6000 rpm. These holes are then taped with threads for attachment with shaft of the hydrofoils. All machining dimensions are determined according to engineering drawings of the part.

Hydrofoils

The hydrofoils, as shown in Figure 4 above, are made out of the extra PVC from the bottom housing. The PVC is to be cut roughly use band saw to three pieces for each of three hydrofoils. Each of the small pieces is then milled to shape with CNC machine with a 3/8" mill bit at a cutting speed of 1200 rpm. There will be one hole drilled by drill press with a 1/4" drill bit at a cutting speed of 1200 rpm on the

same face for each of the three hydrofoils for attachment with the hydrofoil shafts. All machining dimensions were imported into BobCAD to make the CNC g-code.

Keying Process

The output gear and output shaft, both purchased, need to be keyed so that they do not rotate relative to one another. To do this process, the output gear must first be broached. Next, the output shaft needs to be milled so that key stock can be slid between it and the gear. The output shaft should be machined from the top to 1 inch down with a cut depth of .2 inches.

Adapter

The adapter connects the input gear to the motor shaft. To create this, first cut a 1 inch segment of 3/8 inch aluminum. Then use the lathe with a cutting piece to lathe the outside down to 1/4 in for a 1/2 inch segment. Next, drill a .25 inch hole into the opposite side of the aluminum stock to a depth of 3/8 in.

Assembly

The assembly of our parts takes a great deal of time, but is not very risky. Common sense and safety should be taken into considerations throughout all parts of assembly. Many of the parts are fastened together with screws. There are two main sub-assemblies, the top and hydrofoil sub-assemblies, which are combined to create the final assembly.

Top Sub-Assembly

The top sub-assembly includes a DC motor, motor casing, input gear, transmission gear, output gear, output shaft, the double seal flanged ball bearing for the output shaft, the output shaft collar, the dowel pin for the transmission gear, two ball bearings for the dowel pin, the top housing, the bottom housing, weather stripping tape, eight (8) screws. Below, Figure 15 shows an assembly view of the gear box.

This sub-assembly was put together using the following steps.

1. Press fit the output shaft's smooth end through double seal flanged ball bearing to 1.3 in. Figure 18 shows this assembly.

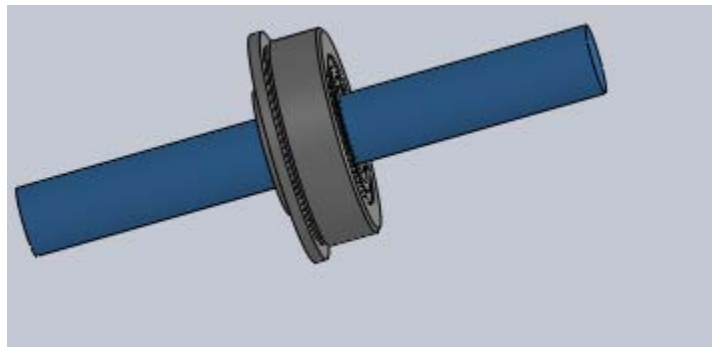


Figure 18: Output Shaft Press Fit to Double Seal Flanged Ball Bearing

2. Connect output gear with the bottom housing and the output shaft. First, press fit smooth end of the shaft through the output gear until the end of the shaft is aligned with top of gear. Next attach a 3/8 in collar to the shaft contacting the top of the bearing. Then insert to key between the gear and shaft so that no rotation occurs relative to these to pieces. Next, press fit the ball bearing on the output shaft into bottom housing with output gear inside the housing wall. Then, place the output shaft collar on the output shaft where flange of the bearing locates. This assembly is shown in Figure 19.

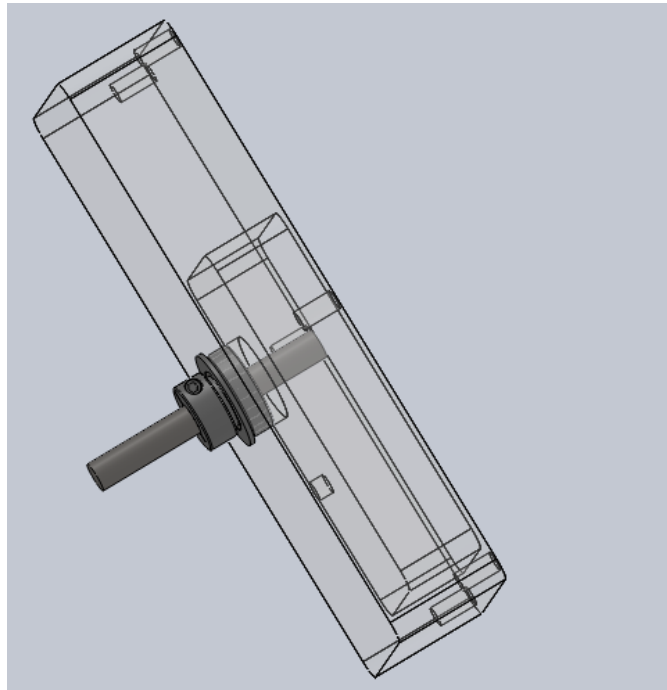


Figure 19: Shaft and Bearing Attached to Housing

3. Connect input gear with top housing and DC motor. First, press fit the adapter into the input gear. Then, use a set screw to attach the adapter to the motor shaft. Next, put the shaft of the motor through the top housing and put in the two screws to secure it. Then, place the motor casing over the motor and glue with epoxy. This assembly is shown in Figure 20.

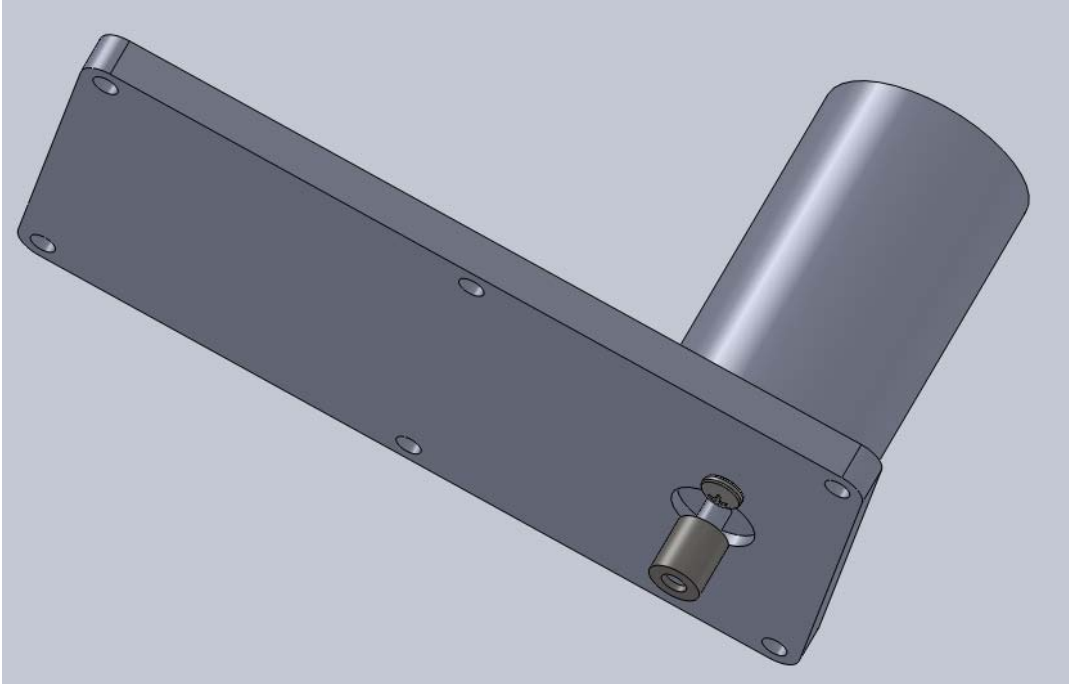


Figure 21: Motor Attachment to Top Housing

4. Place the transmission gear into the bottom housing. First, press fit the two ball bearings onto the transmission gear. Next, press fit the dowel into the two ball bearings within the gear. Then, place the dowel pin for the transmission gear into the slot on bottom housing and carefully match up the teeth of the output and transmission gear. Figure 22 shows this assembly.

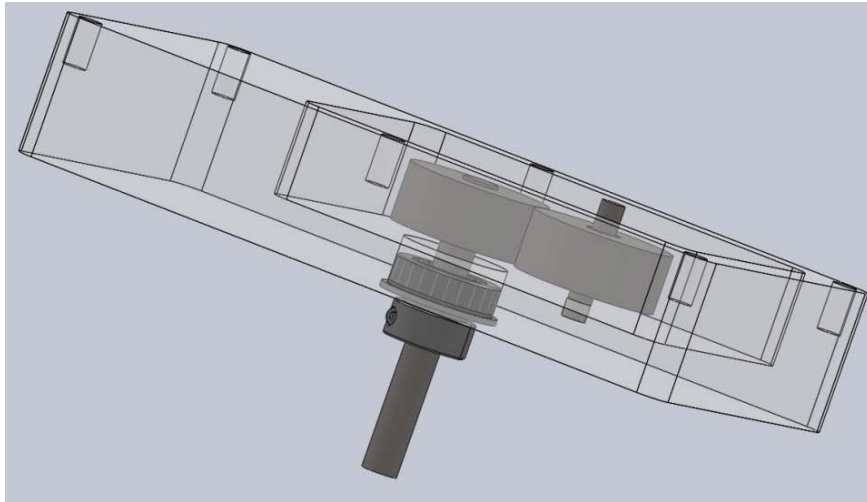


Figure 23: Assembly of Transmission and Output Gear

5. Connect the top and bottom housing. First, place a layer of weather stripping tape over the outer edges of bottom housing. Next, carefully place the top and bottom housing together. Make sure the teeth of transmission gear are matching up. Make sure the dowel pin for transmission gear is placed into the slot on top housing. Make sure the holes for screws are

aligned. Then, place the six screws in their spots to close the gear box securely. This assembly is shown in Figure 24.

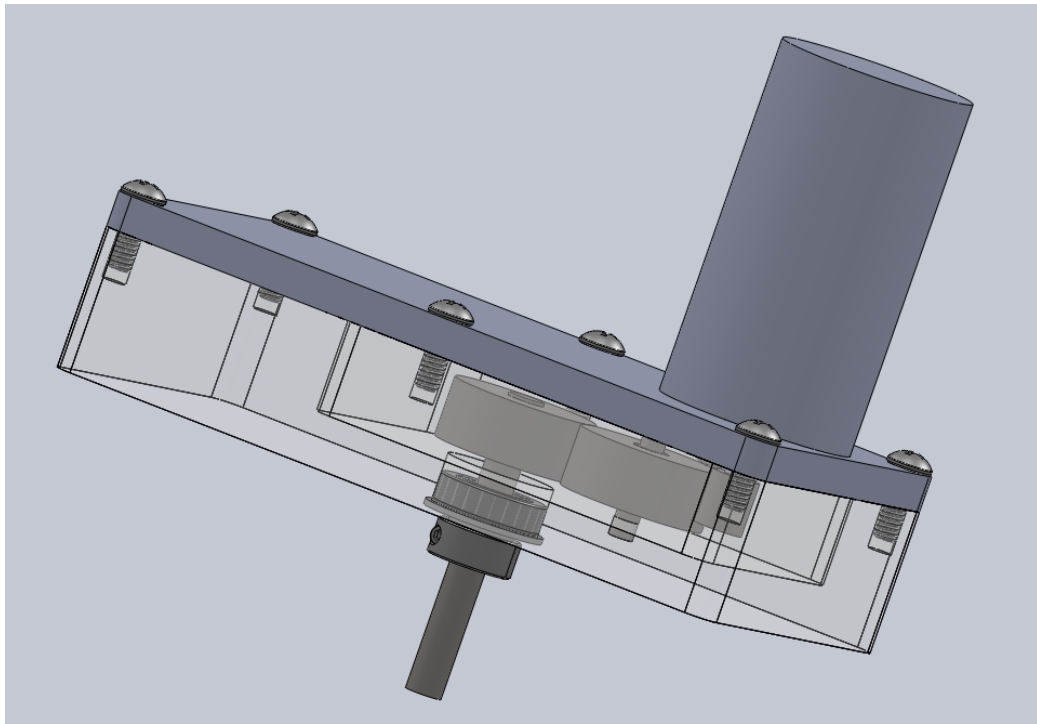


Figure 24: Completed Top Assembly

Hydrofoil Sub-Assembly

The hydrofoil sub-assembly includes three hydrofoils, three hydrofoil shafts, three shaft collars, six nuts, and one hydrofoil hub. Figure 16 shows an exploded assembly view of this.

1. Connect each of the three hydrofoils with each of the three hydrofoil shafts. First, place one of the threaded ends of the hydrofoil shaft into the hole on hydrofoil and go all the way through to the other end of the hole. Next, place a nut on one end of the shaft that already went through the hydrofoil. Then, place a shaft collar on the shaft so that hydrofoil could not slide off the shaft. Use same procedure for all three hydrofoils and shafts. Figure 25 shows this assembly.

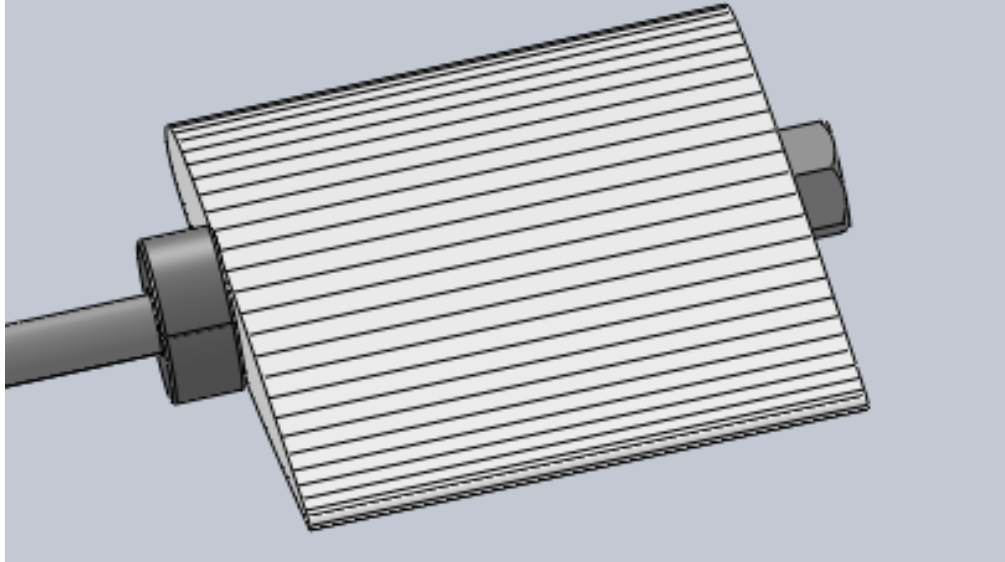


Figure 25: Assembly of Hydrofoil on Hydrofoil Shaft

2. Connect each of the three hydrofoil shafts with the hydrofoil hub. First, put a nut on the empty end of the shaft until the top of the threads. Next, place the empty end of one of the shaft into one of the threaded hole of the hub. Then, turn the shaft until the screw is tight. Finally, turn the nut until it's against the surface of the hub tightly. Use the same procedure for all three hydrofoils shaft. Figure 26 shows this assembly.
3. Modify the hydrofoil to a desired angle of attack. First, turn the hydrofoil until it has a desired angle of attack. Next, tightening the nut next to the hydrofoil until hydrofoil is unable to turn. Use the same procedure for all three hydrofoils and shaft. Figure 26 shows this assembly.

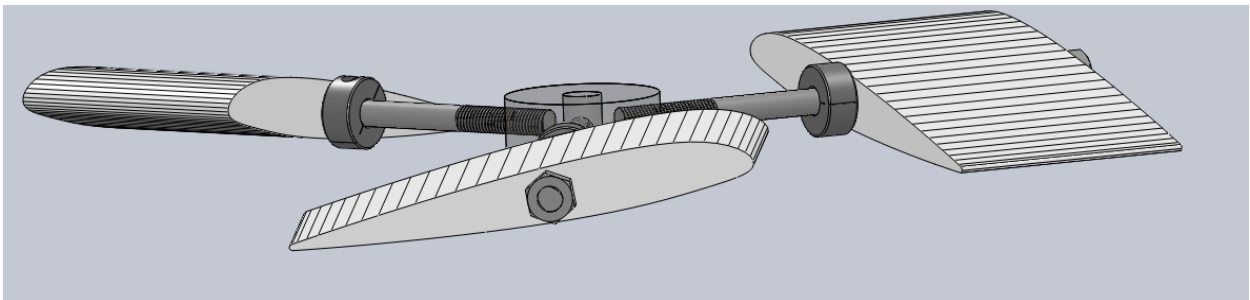


Figure 26: Attachment of Hydrofoil Shaft to Hydrofoil Hub

Final Assembly

Attach output shaft to hydrofoil hub and tighten securely. The final assembly is shown in Figure 27.

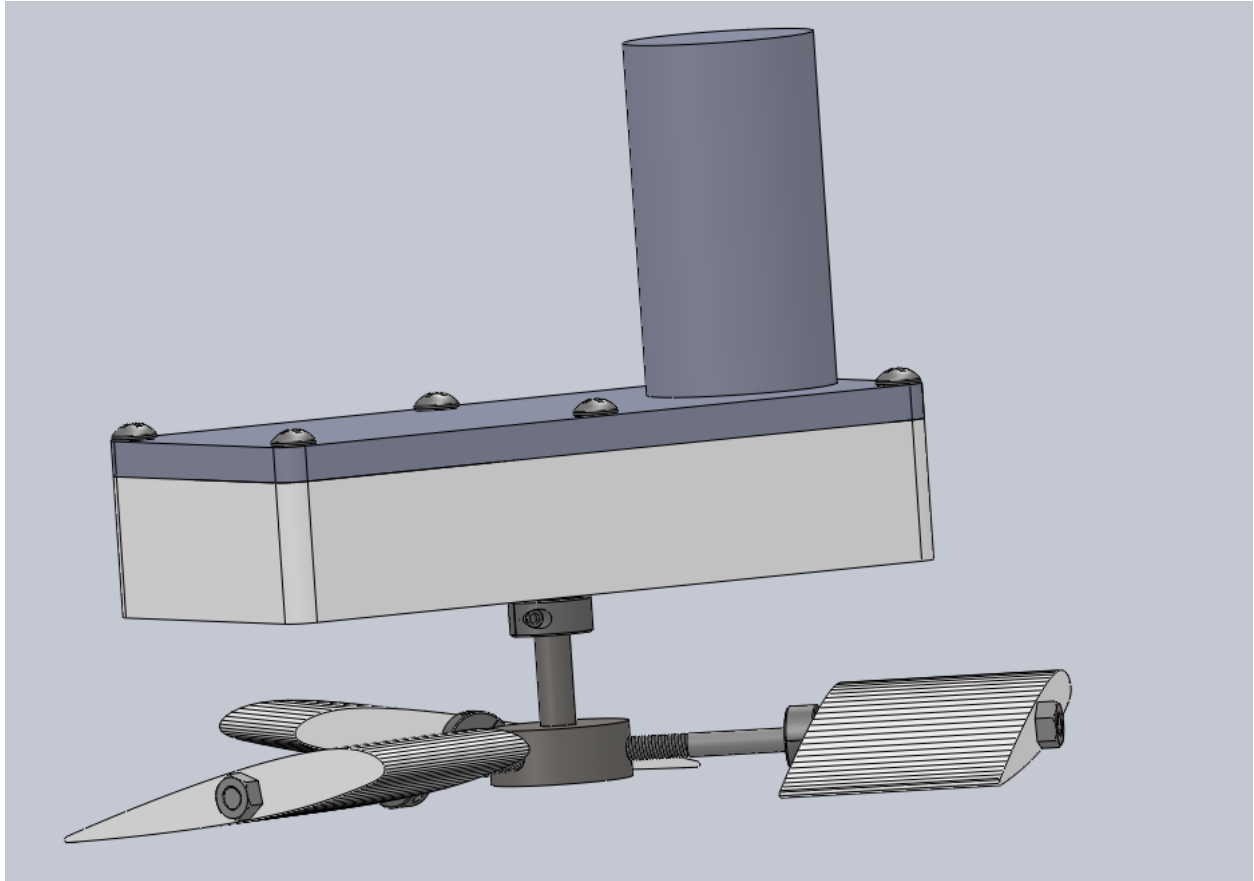


Figure 27: Fully Assembled Hydrofoil Shoe Prototype

After the prototype is assembled, the motor will be wired to the motor controller. The wiring used is provided by the university. The motor controller will be wired to the power source, and a potentiometer will be used to control the speed.

10. VALIDATION PROCEDURE AND RESULTS

In order to verify that our design meets the engineering specifications which defined our project, we must conduct validation procedures. We will conduct simple testing during assembly to assure that the parts are in working order. Once the prototype is complete we will conduct experiments in order to determine the lift and stability of our device.

Experimentation Plans Prior to Design Completion

There was no in-depth testing prior to completing the prototype. There were, however, minor component checks during the assembly process.

As it was installed the gear train was tested to ensure the quality of connection between neighboring gears. This testing was conducted by manually rotating the output shaft and observing the rotations of the gears.

Prior to installation the motor and motor controller were tested to ensure that they have been received in working order. The power supply was connected to the controller and the controller in turn was connected to the motor. Voltage from the power supply was gradually increased and the motor was observed to rotate properly. This confirmed the working of the motor and controller.

Final Testing Procedure

All of the major testing for our design was conducted after the prototype had been assembled. The primary goal of our testing was to establish the maximum load that the shoe can support. Additionally, we sought to determine the general operability of the device, the relationship between motor speed and lift and the stability of the device at the air-water interface.

The first stage of testing was intended to determine the general operability of our device. This means that we confirmed that a voltage applied to the motor will result in rotation of the hydrofoil blades. The initial test can be conducted at a low speed, outside of water. A low starting speed is essential due to increasing stress on the components with increasing angular velocity. The low speed test should be conducted with the device hanging from the fixture inside the plastic container.

After each sequence of tests the device should be inspected to ensure that no parts are loose and that no cracks have formed in the hydrofoils. This inspection routine will prevent a surprise failure to due cyclical fatigue of the parts. If cracks are noticed in the regions of the hydrofoil surrounding the connecting rod, tests will be discontinued.

Testing of the apparatus takes place within a Sterilite 1865 90-quart storage container as pictured in Figure 28, below. The storage container should be filled with water to such a depth that the hydrofoils will be submerged with at least five inches of space between the blades and the bottom of the container. The rigid plastic container serves both to hold the volume of water in which the test will occur and provide a safety barrier between the operators and the device. In addition to the side walls of the container, a plastic cover can affix to the top in case of any parts ejecting from the device vertically. The cover also prevents any splashing on the floor of the lab. A hole was cut in the cover in order to allow wiring and the support rods to pass through.



Figure 28: Sterilite storage container

The purpose of the testing fixture, pictured in Figure 29, is twofold. Firstly, it is necessary to restrict the motion of the shoe to one (vertical) degree of freedom. If the shoe were unrestrained the motor would cause the top of the shoe to rotate in opposition to the blades. By fixing the shoe (a) we simulate the resisting torque that would be supplied by the user's leg. The second purpose of the fixture is to provide a means of measuring the lift force produced by the device. By reading the load applied to the spring force gauge (b) we can determine the lift transmitted through the connecting rods (c).

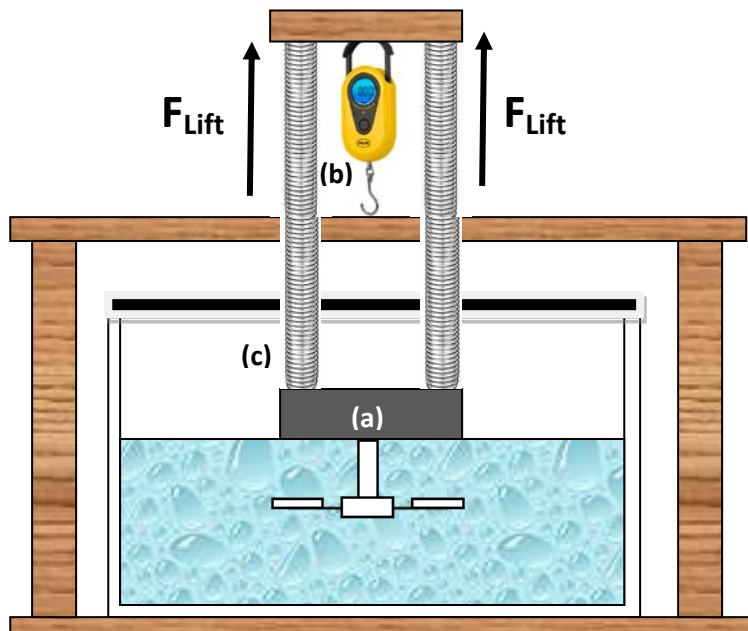


Figure 29: Schematic of testing setup

The plastic container should sit on the floor of the lab while the power supply remains elevated on a table to ensure that no water is splashed onto the power supply.

Starting with the lowest voltage that will cause rotation of the blades, input voltage is increased in 2 volt increments and the corresponding lift force and current needed is recorded. At each voltage, a video was also taken to determine the angular velocity. To determine the angular velocity, the amount of frames was recorded that it took the blades to rotate one revolution. Knowing that the video recorded at 30 frames per second, the angular velocity was then determined. Along with each one of these data points, qualitative observations are made (e.g. notes on turbulence, stability of the machine).

Safety protocol for testing

Throughout the testing procedure, the team must remain vigilant in order to minimize any safety concerns. The primary safety concern associated with the test is the possibility of rotor parts failing and being ejected from the spinning assembly. The plastic enclosure serves to mitigate any danger of flying parts so it is essential to enclose the device in the container before the motor is operated. This safe working protocol is noted in the “Safe working procedure checklist”, Table 2, below.

Table 3: Safe working procedure checklist

	Safety glasses must be worn throughout testing
	Shirts must be tucked in, sleeves rolled up
	Only operate device while it is safely enclosed in the container
	Do not touch the wire leads while the power supply output is on
	Turn power supply to “Output Off” before making any adjustments
	Stand clear (at least 8’) of container while test is running
	Do not touch water while power supply output is on

Another possible area of concern during testing is the presence of electrical devices in the vicinity of water. The working voltage of the motor is 24 V DC. This presents significantly less danger than mains voltage, however extreme caution still must be taken to avoid hazards. Before using the device one should ensure good connections at the motor electrodes that will not detach through vibration of the device. To avoid any possible electrical hazards, team members should not touch the device at all when it is powered and in the water. It is possible to control the motor remotely by using the power supply and control circuit.

Validation Results

The validation testing was performed on the morning of December 12th, 2009 in Professor Chronis’ lab. The device was first set into the fixture and connected to the power supply. Before adding water to the container the device was tested in air. This was done to ensure that the direction of rotation was correct and that the power supply was connected properly. The device was run at several different voltages and was observed to rotate properly. No lift was recorded in air.



Figure 30: The hydrofoil shoe running in the test rig

Water was next added to the container until it reached the bottom of the PVC block. The water was warm and clean. The container cover was secured and the hydrofoils were started rotating at a low speed.

As the rotor speed was increased a rotating vortex of water was clearly observed to be rotating along with the blades.

Significant turbulence within the container was observed at all rotor speeds. The small size of the container (32" by 18") resulted in waves bouncing off of container walls and interfering with each other creating a choppy surface.

Throughout the experiment no lift was recorded on the force gauge. The gauge was later removed and the presence of lift force was manually tested by pulling on the sliding rods in the fixture. The manual testing showed no observable lift. The experimental data recorded can be found in Figures 31 and 32 and Table 4 below.

Figure 31: Velocity versus input voltage in air and water

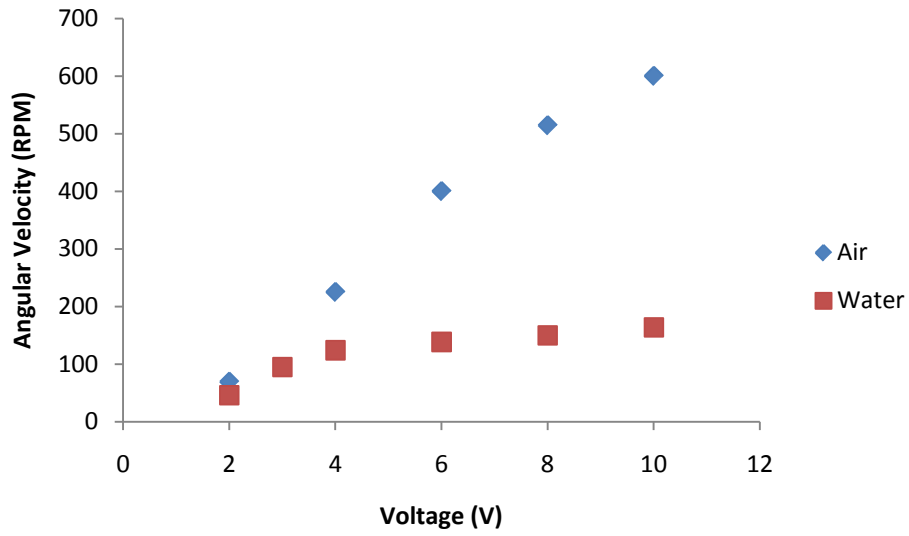


Figure 32: Current versus input voltage in air and water

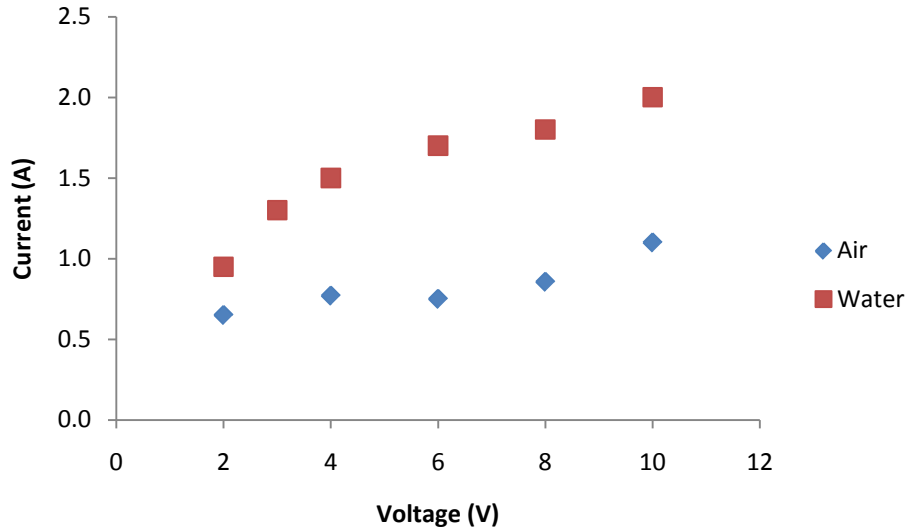


Table 4: Experimental Test Results

In Air			In Water		
Voltage (V)	Current (A)	RPM	Voltage (V)	Current (A)	RPM
2	0.95	46	2	0.65	69
3	1.30	95			
4	1.50	124	4	0.77	225
6	1.70	138	6	0.75	400
8	1.80	150	8	0.86	514
10	2.00	164	10	1.10	600

The amperage seen on the power supply readout was significantly higher than expected and often above the rated specifications of the motor. As the gauge of wire leading to the motor was of sufficient size we determined it to be safe to push the motor to its limits. At the conclusion of the experiment we raised the voltage across the motor until it reached 26 Volts. The resulting 7 Amp current burned out the motor leading to failure.

11. DISCUSSION

The validation results showed that the selected design was not capable of producing the expected lift. Although the engineering calculations predicted a supported load of greater than 20 kg there are many possible contributing factors for the unexpected results. These factors include: greater drag than expected, tip losses, vortex effects and container turbulence.

As detailed in the engineering analysis section lift and drag calculations were based on formulas derived from the equations used for linear motion of an airfoil. A more rigorous analysis of the specific rotary situation would have entailed three-dimensional computational fluid dynamics models. Such modeling was beyond the scope of this project.

Greater drag

The maximum angular velocity of the rotor blades was approximately half of the expected value. As lift grows with the square of the velocity this translates to a fourfold reduction in lift. As a sufficiently high velocity was observed while testing in air, the limiting factor must be the drag experienced in water.

Our original drag calculations predicted a drag torque of 0.753 N-m. The actual drag was on the order of four times as large judging by the accompanied reduction in angular velocity. Additional possible sources of drag that were unaccounted for include drag for the non-airfoil shape of the connecting rods, rotor hub and acorn nuts on the outside of the blades.

A small amount of cavitations was observed as bubbles forming on the trailing edges of the hydrofoil blades. These low pressure pockets introduce greater drag and interference with the flow motion that is not accounted for in the simple drag and lift equations.

Drag could be reduced by utilizing thinner hydrofoil blades and streamlining other rotor components (connecting rods, nuts, etc.) to minimize losses there.

Tip losses

An untapered wing design can result in vortices at the wing tips [33]. These vortices lead to interference drag caused by a pressure drop behind the wing. The squared edge of the hydrofoils used here may have led to significant tip losses.

Tip losses could be mitigated by encircling the rotor blade tips in a stationary housing. This feature could be incorporated into the safety cage discussed in final design plans.

Vortex effects

As the hydrofoil blades were rotating a vortex of rotating water was observed to be moving along with the blades. This is due to the boundary layer of water matching the speed of the blade.

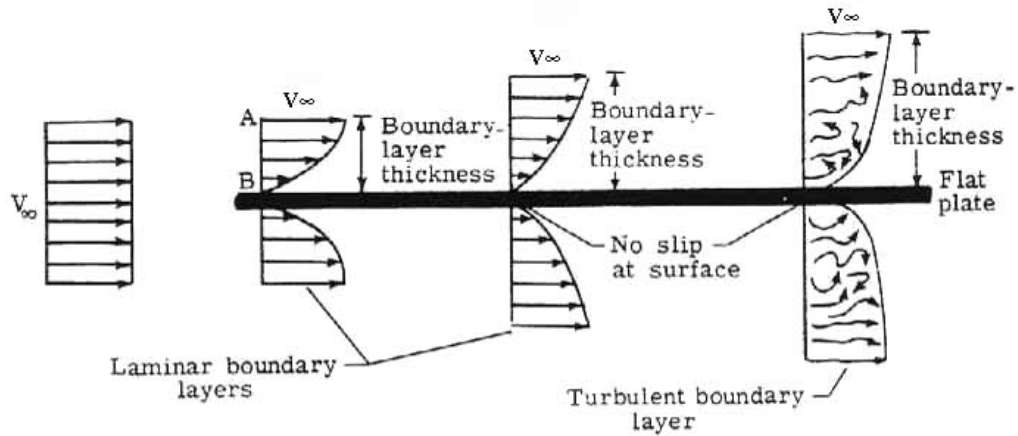


Figure 33: Boundary Layer Effects on a Flat Plate [34]

The rotating vortex of water tends to match the speed of the rotor blades. When this occurs, the relative speed of the wings to the water decreases:

$$V_{relative} = r\omega_{rotor} - r\omega_{vortex} \quad (\text{Eqn. 15})$$

Stream velocity of the fluid over the airfoil is the velocity that induces lift. The vortex motion of the water decreases the relative stream velocity and thus the lift. The closer the stream velocity matches the rotor velocity, the further lift will be reduced.

The most effective way to reduce vortex circulation about the rotor would be to reduce the drag of the airfoils. This could be achieved by making thinner blades. Another possibility would be changing the blade materials and using two instead of three.

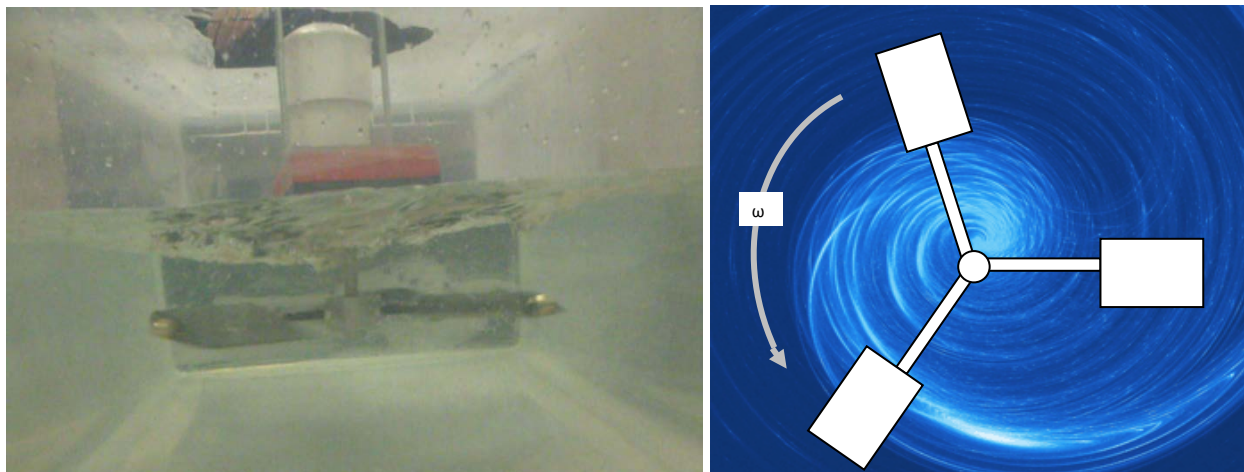


Figure 34: Photograph and Diagram of Vortex about the Rotor Assembly

Container turbulence

As the testing enclosure was small relative to the size of the rotor (~2 times wider) significant turbulent interference was observed as waves bounced off of the container walls. This interference introduces non-uniformity into the flow patterns of the water. The non-uniform flow results in vibrations in the rotor structure and imbalance in the relative lift of the wings.

12. RECCOMENDATIONS

Based on the results of our validation testing we recommend that the rotary hydrofoil concept is developed more fully to determine any validity. Failing this, it is recommended that other means of surface locomotion are explored. Our concept generation efforts covered a broad range of possible mechanisms to support a human's weight on water. There is, however, a seemingly endless list of possibilities and one of these may prove more fruitful than our own efforts. We thus recommend that a future student team is given the same task to start from scratch and design their own mechanism for surface locomotion. Especially of interest are options of some sort of sold-state device that use advanced materials in some way to support the user's weight.

13. CONCLUSION

This project's overarching object was to create a device allowing humans to walk on water. The purpose of this device, within the scope of the project, is for recreational use. Our specific design targeted a 10-12 year old child that weighs approximately 40kg. Many ideas were considered using concepts from buoyancy to surface tension to a biological approach. The design that we settled on was a rotational hydrofoil device. The concept is that rotating hydrofoil blades spin through the water at a high velocity to generate lift capable of supporting a walker. It consists of one shoe for each foot and uses a control system to help keep the user balanced. The shoe would be powered by a LiFePO₄ battery pack and use a speed controller to control the lift generated. The prototype that was actually fabricated consisted of only one shoe and no control system. It also used a power supply instead of battery due to budget constraints. Our prototype did not perform as expected. No lift was generated during our validation tests. Lack of lift generation could be due to more drag being produced than expected, vortices produced that caused a lower relative speed of the water to the hydrofoil and other losses due to reasons such as vibrations and instability. Through further testing and more rigorous fluid analysis this design can be improved and it can be determined whether it is a viable concept. If the concept does not prove viable we have laid forward a wide range of alternate concepts that can be pursued in the continuing effort to make a human water shoe.

Acknowledgements

We would like to thank our sponsor Professor Chronis for his support throughout the conception, design and validation of this project. Additional thanks are owed to Bob Coury and Marv Cressey for their assistance throughout our machining process and Dan Johnson for his help on a huge variety of issues related to the project.

APPENDIX A: Bill of Materials

Part Name	Part Number	Vendor	Price	Quantity	Total Cost
Acrylic	<u>8560K591</u>	McMaster	\$14.29	1	\$14.29
Flanged Ball Bearing	57155K3030	McMaster	\$6.38	2	\$12.76
Two-Piece Shaft Collar	9520T2	McMaster	\$5.58	3	\$16.74
Motor	BDS-52-85-24.0V-5450	Anaheim Automation	\$59.70	1	\$59.70
Transmission gear	<u>6325K65</u>	McMaster	\$23.98	2	\$47.96
Speed Controller	MBDC050-024031	Anaheim Automation	\$29.00	1	\$29.00
Motor output gear	<u>6325K31</u>	McMaster	\$12.03	1	\$12.03
Ball Bearing	57155K355	McMaster	\$6.00	2	\$12.00
Dowel Pin	97395A492	McMaster	\$7.73	1	\$7.73
Output shaft	97042A352	McMaster	\$6.53	1	\$6.53
Housing Ball Bearing	<u>6384K358</u>	McMaster	\$6.21	1	\$6.21
Hydrofoils Shaft Collar	<u>6435K12</u>	McMaster	\$1.98	3	\$5.94
Threaded Rod	<u>90281A100</u>	McMaster	\$1.67	3	\$5.01
Shaft Collar	6157K13	McMaster	\$2.36	1	\$2.36
.375 Shaft Collar	2AKW2	Grainger	\$2.89	3	\$8.67
.250 Shaft Collar	2AKX5	Grainger	\$3.24	1	\$3.24
Double Threaded Rod	3FA80	Grainger	\$6.93	2	\$13.86
PVC Cap	NA	Grainger	\$2.84	1	\$2.84
PVC Tubing	NA	Wolverine Supply	\$13.36	1	\$13.36
Spacers	NA	Grainger	\$1.98	1	\$1.98
J-B Weld	NA	Grainger	\$5.99	1	\$5.99
Threaded Rod	2FGK3	Grainger	\$2.11	2	\$4.22
Motor Screws	NA	Carpenter Brothers	\$0.23	4	\$0.92

Screws	NA	Carpenter Brothers	\$0.45	3	\$1.35
Weather Stripping	NA	Carpenter Brothers	\$0.00	1	\$0.00
Aluminum Stock	NA	Bob's Shop	\$0.00	1	\$0.00
PVC Stock	NA	Bob's Shop	\$0.00	1	\$0.00
Nuts and Bolts	NA	Bob's Shop	\$0.00	1	\$0.00
Washers	NA	Bob's Shop	\$0.00	1	\$0.00
Tape, Adhesive, Lubricant	NA	Bob's Shop	\$0.00	1	\$0.00
Shipping					\$20.00
Tax					\$18.10
Total					\$332.79

APPENDIX B: Engineering Changes

1. Transition gear bearing changed from regular ball bearing to flanged ball bearing.

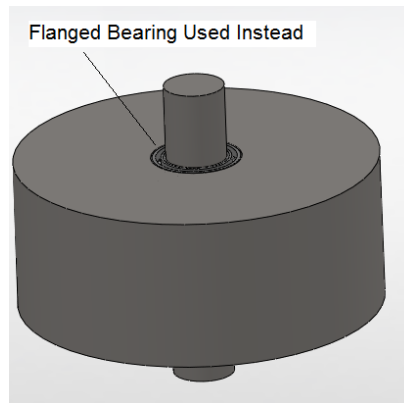


Figure 35: Transition gear on bearings

The regular bearing was changed to a ball bearing due to a recommendation from Bob Courey. The press-fitting machine would not work on a bearing that small without a flange. In addition to that, the flanges prevented the bearing from moving vertically. This made our gears more stable.

2. Spacers added between motor and top housing over around 4 screws.

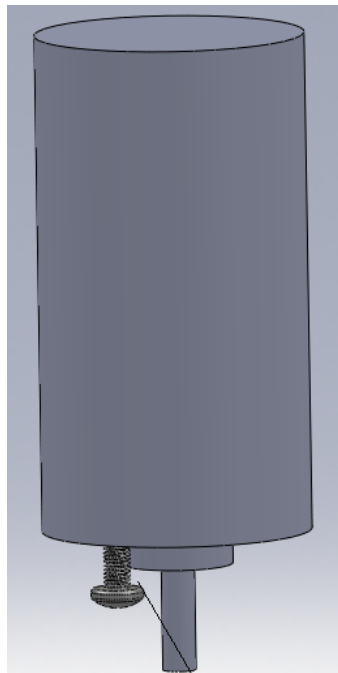


Figure 36: Spacer placement

Four hollow cylindrical spacers were added to separate the motor from the top housing. One was placed over each screw. The purpose of this is to align the input gear with the transition gear properly. This was suggested by Bob Courey.

3. Adapter to connect input gear to motor.

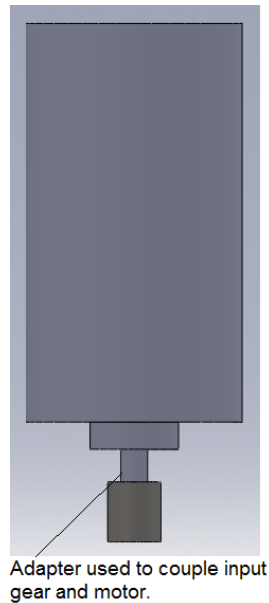


Figure 37: Motor output adapter

An adapter was needed to connect the input gear to the motor shaft. The reason for this is because the machine shop did not have tools that could machine a key in the input gear due to its small size. The adapter was suggested by Bob Courey. The adapter was press fit onto the gear and set screwed into the motor shaft.

4. Output gear and output shaft keyed to prevent movement.

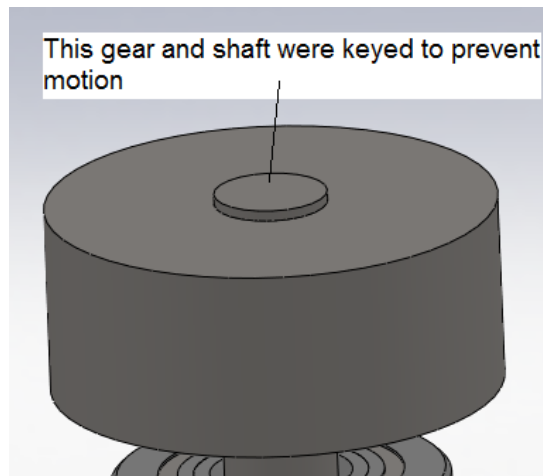


Figure 38: Keyed gear on shaft

The output gear and output shaft needed to be keyed because they were not able to be press fit together. The output shaft was slightly smaller than the specifications said. Bob Courey suggested this change. The keying prevented motion of the gear relative to the shaft which accomplished the same thing as press fitting.

5. Nut added to hydrofoil hub to prevent vertical translation.

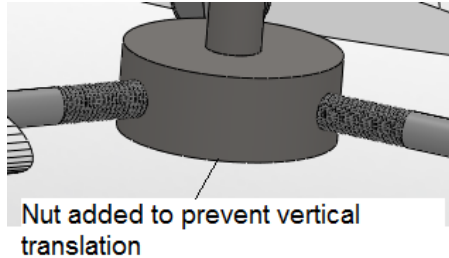


Figure 39: Rotor hub

A nut was added to the bottom of the hydrofoil hub to prevent vertical translation. This was suggested by Bob Courey. When the system accelerated the hydrofoil would have the tendency to tighten, and a nut would not be needed. When the hydrofoil system slowed down, there would be a torque on the hydrofoil hub in the opposite direction causing it to loosen and eventually fall off. A nut was added to stop this movement.

6. Extra collar added to output shaft to prevent motion.

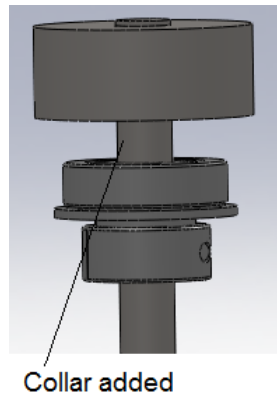


Figure 40: Extra collar position above center bearing

Another collar was added to the output shaft on the other side of the flanged bearing to prevent downward motion. This was suggested by Bob Courey. With the original setup the shaft was constrained from moving upward but not downward. The new setup prevents all vertical motion.

APPENDIX C: Design Analysis Assignment

Material Selection - Functional Performance

Multiple materials were used for our device. Here are two components analyzed for their material usage.

Bottom Housing

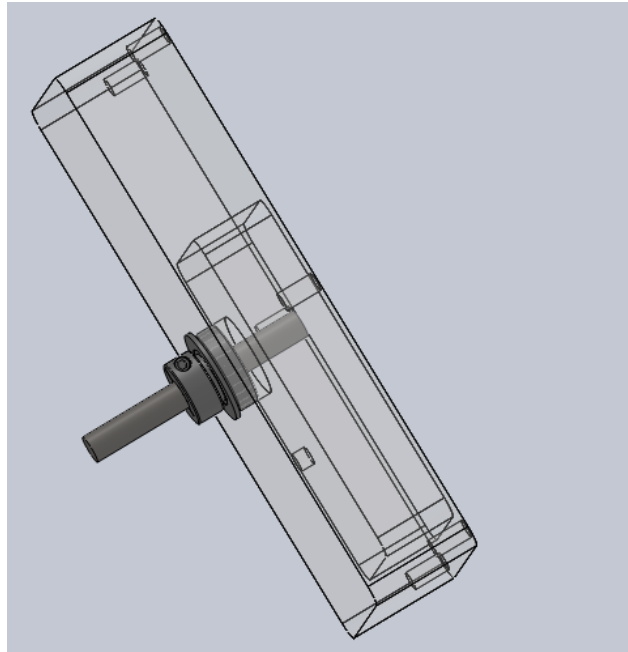


Figure 41: Bottom Housing

The function of bottom housing is to contain the gear trains and provide a stable base for the system. It is also used to support the user's weight. It has to be strong in order to support the weight and stress. It has to be light so the device doesn't need to generate too much extra lift to compensate. It has to be water proof and rust resist so the gear train and motor don't get wet and it doesn't rust over time. It has to be easy to obtain and has a relatively low cost. It also has to be easy to machine in order to save time during manufacturing. The material we decided to use for this part is PVC Type I. PVC has a yield strength of approximately 40 MPa and a impact strength of approximately 9 J/cm, which is enough for our design according to the calculation. The one major deciding factor for pick PVC is its availability; they are stocked at Bob's shop. This also means the PVC is free, lower the total cost of the device. PVC has a density of 1.4 g/cm^3 , which is relatively low. PVC is well known for its high machinability. PVC is also widely used for water pipes; this shows its satisfactory water sealing ability and rust resistance.

Hydrofoil Shaft



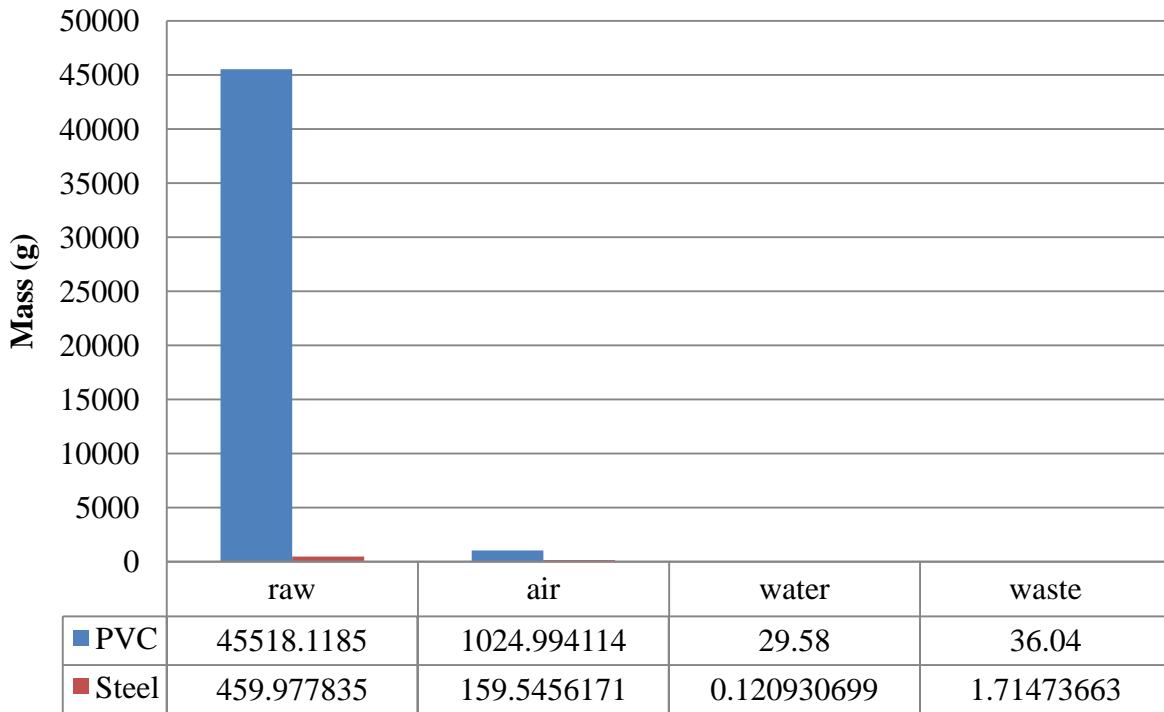
Figure 42: Hydrofoil Shaft

The function of hydrofoil shaft is to connect hydrofoil hub with the hydrofoils and support the entire device and the user. It has to be strong in order to support the weight and stress of the user and the device itself. It has to be easy to obtain and has a relatively low cost. It has to be rust resist due to the device going to operate in water. It also has to be easy to attach with hydrofoil hub and hydrofoil. The material we decide to use is stainless steel. It has a yield strength of 900 MPa, which is well over the calculated strength needed. It cost \$1.67 per piece at McMaster-Car, which is relatively cheap. Stainless means its rust resistance is high. It also come with threaded ends for easy attachments.

Material Selection - Environmental Performance

For above mentioned two materials, PVC and stainless steel, the environmental impact will be analyzed. The approximated mass needed for both PVC and stainless steel is 0.5 kg and 0.15 kg respectively. The mass of raw material, air emission, water emission, and waste are shown in figure below.

Figure 43: Mass of emissions for both PVC and Steel



As observed in table, one major emission category is raw material. After look into data of raw material, it is determined that cooling water plays a major role in raw material of both PVC and steel, approximately 97% of raw material for PVC consisted of cooling water and 40% for steel. Second relatively large emission comes from air. It is determined that carbon dioxide is one main emission for both PVC and steel in air, consisted of approximately 97% for PVC and 95% for steel. Water and waste emission is negligible compare to raw material and air. Overall, PVC has creates more impact to environment than steel.

When looked at impact on human health, ecotoxicity, and resources, both PVC and steel are evaluated. The result can be seen in Figures 44, 45, and 46 constructed through SimaPro. According to this figure, PVC has the higher impact on human health; steel have higher impact on ecotoxicity; and both PVC and steel have some impact on resources. When look at the impact throughout the life cycle of the product, PVC shows a considerable greater impact according to Figure 46.

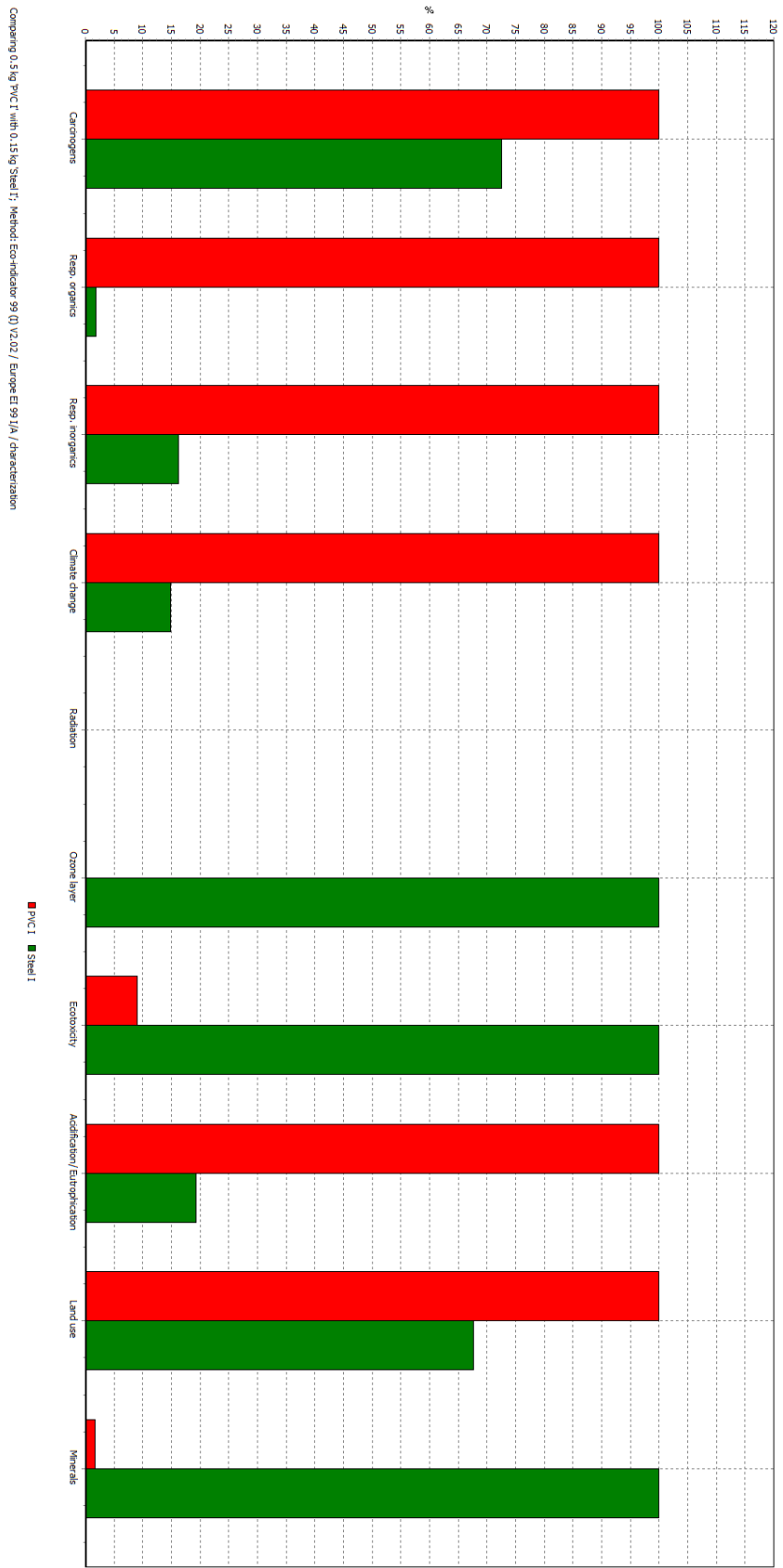


Figure 44: Characterization chart from SimaPro

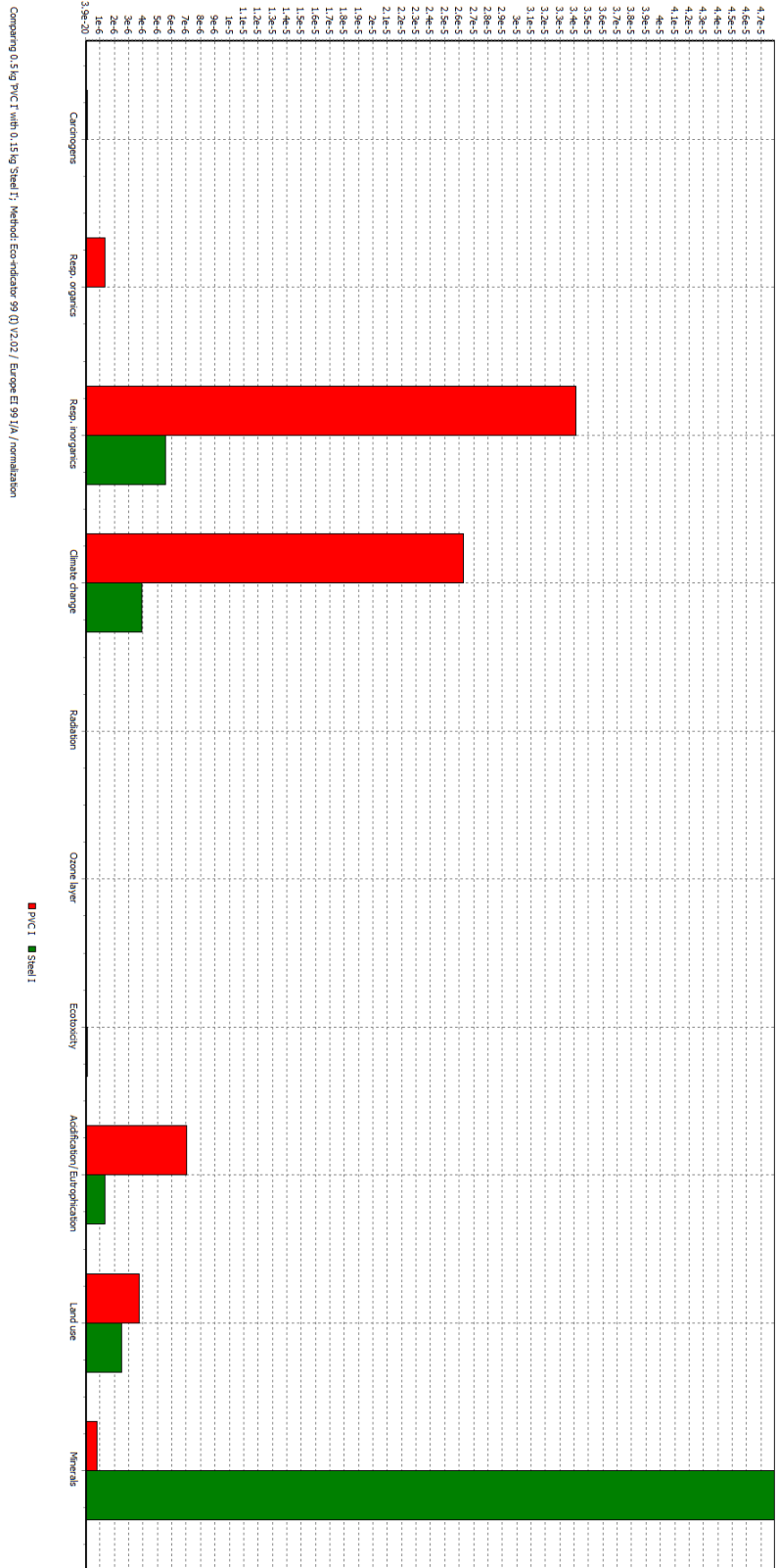


Figure 45: Normalization chart from SimaPro

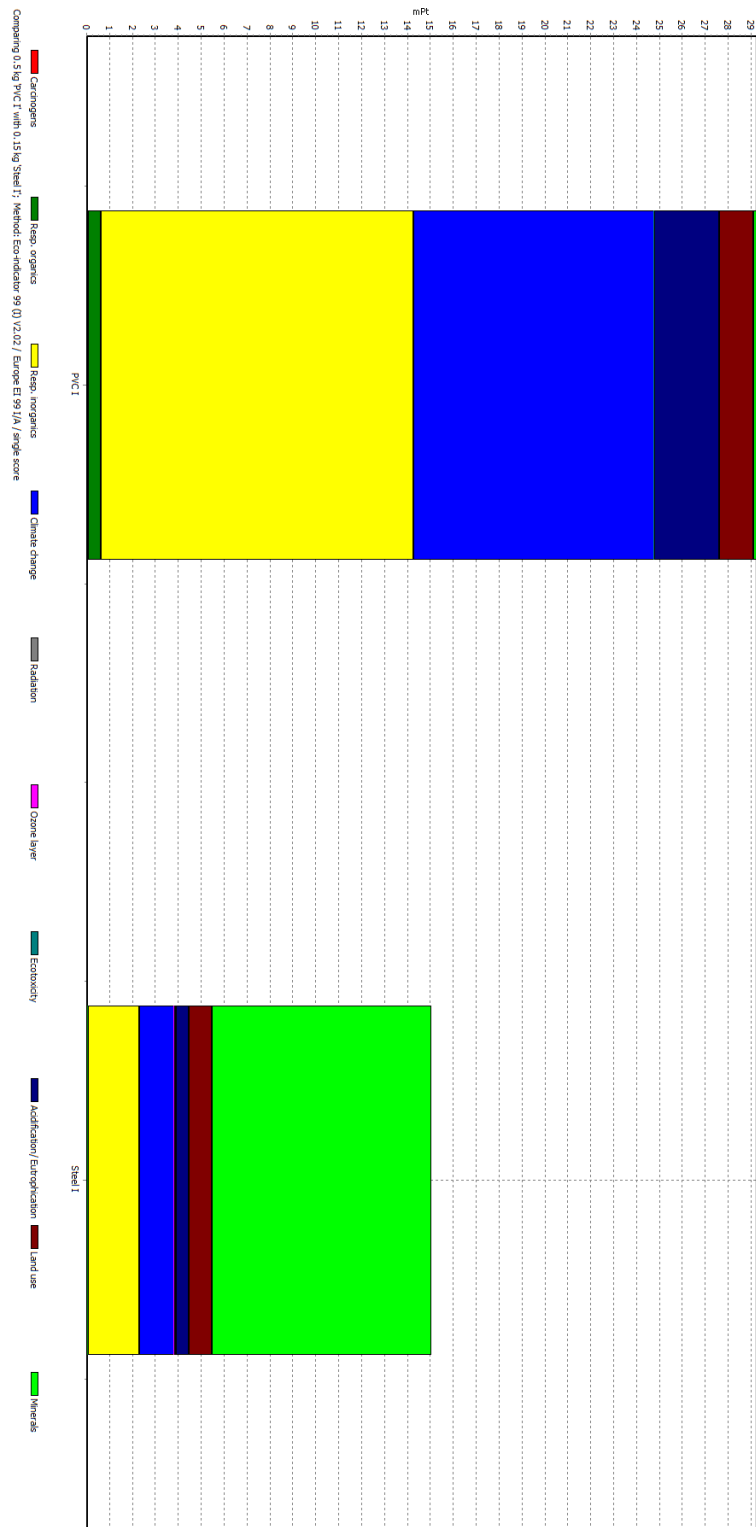


Figure 46: Single Score chart from SimaPro

Manufacturing Process Selection

To determine the batch size, the target market should first be understood. This shoe would be mostly used for recreational purposes at first. The target person is 10-12 years old and weighs less than 40 kg. This product would most likely only be used in fully developed countries due to the electrical needs of the product. The novelty of this product might draw potential buyers, but because a product like this was never mass produced, there may be some hesitation to buy this product at first.

We believe that 100,000 units, or 50,000 shoes, would be a reasonable amount to be sold. The product would also most likely cost between \$100 - \$200 per shoe based on estimates of material cost, labor, and overhead costs based on 50,000 units being sold. The battery would cost an additional \$150, bringing the total cost for two shoes and a battery to \$350-\$550. In order to generate a profit there would also need to be a mark-up.

To manufacture the bottom housing, we believe that injection molding would be the best method. The type of injection molding specifically would be thermoplastic injection molding. The reason for this is because the material used is PVC. This process would be used because of the high production size. The best batch size for injection molding is between 10,000 and 1,000,000 units. We would need 100,000 units, one for each shoe. The size of the shoe and desired roughness is perfect for this shoe. A roughness of 0.04 mil is smooth enough for this application and well within the manufacturing limitations. While the cost of the machinery would be in the range of \$100,000, that cost divided over 100,000 units would only result in a cost of \$1 per shoe. This method is very cost effective for such a large batch size, requires minimal amounts of labor, and can produce the produce within the needed tolerances.

Below is a diagram of what this manufacturing process looks like.

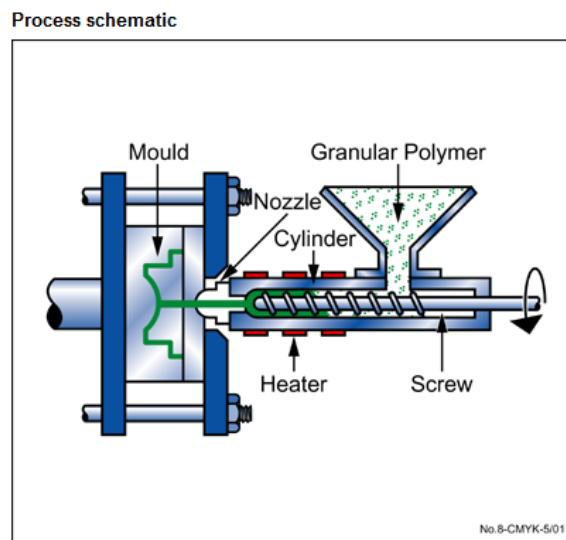


Figure 47: Injection molding diagram
Photo taken from CES software.

The type of manufacturing method used to create the hydrofoil shaft would be CNC, or automated, turning, or lathing. The reason that this method would be used is because the stainless steel shaft is cylindrical. This shape is perfect for lathing. A lathe can produce the desired batch size with a reasonable cost. A lathe can also produce the threads needed on the shaft easier and cheaper than most other manufacturing processes. It can also produce materials at the same rate as the injection molding, which will reduce the need to store excess parts while a different part is made. Like injection molding, the machining cost can be up to \$100,000. Since 100,000 parts would need to be made, this cost alone is only \$1 per part. Below is a photo of what the lathing process looks like.

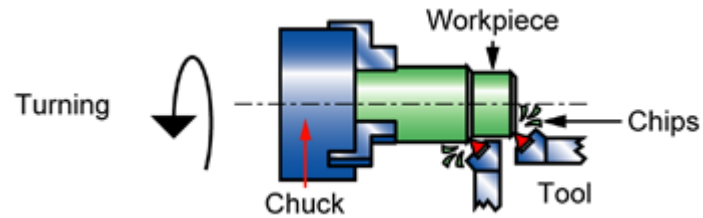
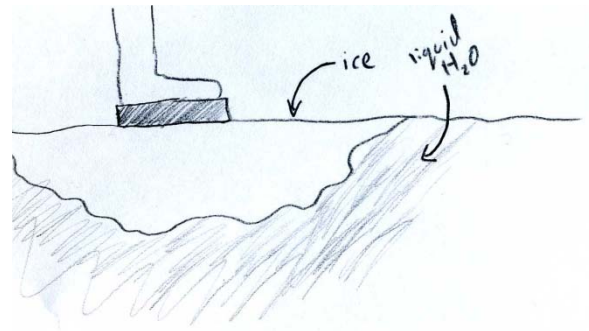


Figure 48: Lathe machining diagram
Photo taken from CES software.

APPENDIX D: Alternative Design Concepts

Water Freezer Shoe

As ice is less dense than water and thus buoyant it can be used to support a load above the surface in the same fashion as a raft [35]. This concept involves freezing the water below the walker to create a series of 'ice rafts' over which he can walk. This would require freezing large volumes of water at very high speeds. One method for such instantaneous freezing of water would be to pour liquid nitrogen into the body of water. This method has the obvious inconvenience of requiring the walker to carry a large quantity of liquid nitrogen. As ice is only fractionally less dense than liquid water the size of the ice raft would have to be on the order of ten times the volume of the walker. Freezing such a quantity of water at high speeds is unfeasible.



Vibrating Shoe

The possibility of a vibrating plate hovering on the surface of the water was discussed as a possible load supporting structure[36]. Further research lent no credence to the idea that a vibrating structure would be supported on the surface. It would seem that the same hydrostatic rules governing a stationary plate apply and vibrating is not a means to achieve flotation.

Human Skipping Catapult

Inspired by the phenomenon of stones skipping along the surface of a body of water, this concept exploits the same effect on a human body. The setup would involve using a catapult to launch a person parallel to the water surface and have them skip along the surface to the other side. Skipping of a stone is made possible by a lift force generated on the stones impact with the water's surface[37]. The lift force is dependent on velocity and angle of attack of the stone[38]. Despite the soundness of the physics behind it this idea was abandoned due to the inherent danger to the person being launched at high velocity.

Helium Balloons

Balloons filled with a gas less dense than air are subject to an upward buoyant force. Helium filled balloons in sufficient quantity could produce an upward force capable of supporting a person[39]. This concept does not require a specific shoe design and would not truly achieve the goal of walking on water but rather hovering over water.

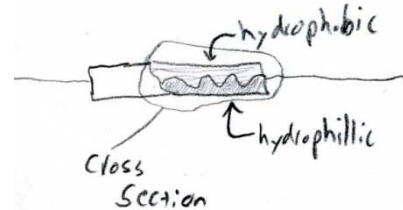
Electrolysis Pressure Reduction Shoe

In the process of electrolysis a voltage difference applied across a volume of water causes the

separation of hydrogen and oxygen molecules, creating bubbles of each gas at the electrodes[40]. These gases, being less dense than water create an upward lift on any surface to which they adhere. The volume of gas produced through electrolysis would not be of significant quantity, however, to result in a large enough buoyant force needed to support our target load.

Hydrophobic/hilic Patterned Internal Perimeter Shoe

A modification of the aforementioned “Internal Perimeter Shoe” this design includes a pattern of hydrophobic and hydrophilic material abutting each other[41]. This is intended to force the contact line of the water to follow this sinusoidal pattern thus increasing the contact area over that of a straight line. The concept is unproven but even if it were to work the limitations imposed by the Archimedes principle rule out the possibility of achieving a sufficient surface tension force.



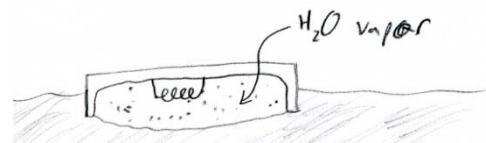
Tentacle Displacement Shoe

The Tentacle Displacement Shoe is based on the propulsion method of a squid, using the motion of many tentacles to displace water and create thrust[42]. This mode of propulsion requires the same displacement rate as the previously described rocket-style thrust and achieves it with a much more complicated and difficult to design mechanism: articulating tentacles.



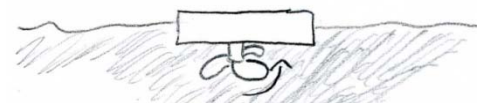
Boiling Water Support

This concept involves heating to a boil the water directly below the shoe. It was thought that boiling water could create sufficient pressure to support a load from above[43]. After review of the idea, however it was realized that this design would be limited to the same constraints as a buoyant shoe, as a pressurized volume of water would escape from the sides of the container as it pushes the water down.



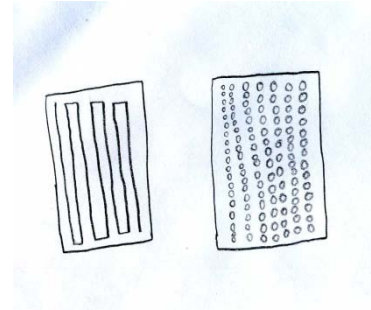
Propeller Shoe

Using the same mechanics that a motor boat uses to generate thrust, this concept redirects that force vertically and uses it to support a load[44]. This system would require a large amount of energy to be supplied to the shoes in some manner and the size limitations would make the placement of any motor or propeller very challenging.



Internal Perimeter Shoe

This design utilizes surface tension to generate an uplift force. The force created by surface tension is directly related with the perimeter of the object contacting the water surface. This design maximizes this perimeter by introducing zigzag lines or many small holes in the bottom of the shoe. The main weakness of this design is that it has to follow the Generalized Archimedes principle. The principle states that the surface tension force supporting an object is equal to the weight of the water displaced to the meniscus[45]. For this design, the shoe size limits the amount of water that will be displaced regardless of zigzag lines or holes within the shoe. Thus, the small shoe size will not create sufficient uplift force.

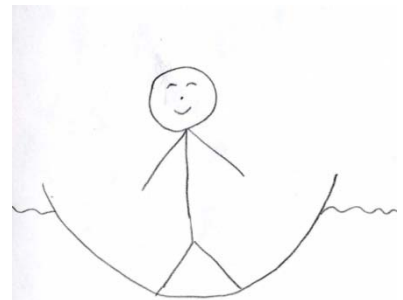


Chemical Shoe

This design utilizes change in water properties to generate an uplift force. The uplift force created by buoyancy in water is directly proportional to water density. The density of the water can be increased with chemicals, such as salt, to produce a higher uplift force[46]. The main problem with this design is the amount of chemicals required to alter the density of water. A huge amount of chemicals would be required to increase density of water by even a small amount. This problem causes this design to be impractical.

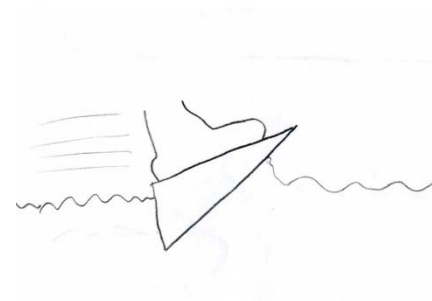
Inverted Umbrella Shoe

This design utilizes buoyancy to generate upward lift. The lift force is created by displacing a large volume of water below the walker. The volume is displaced by introducing a large membrane-like object under our shoe[47]. The membrane can also be designed to be foldable, thus make it easy to transport when needed. The downside of this design is its big size. In order to create sufficient uplift force, the membrane needs to be large enough to displace a volume of water at least equal to the walker's weight. This will give the user a hard time maneuvering and will exceed the project's design specifications.



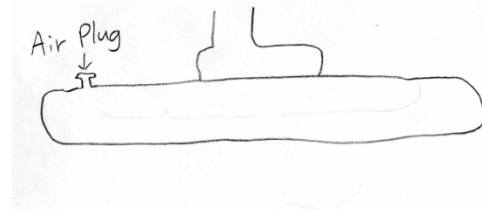
Water Skiing Shoe

This design utilizes high velocity motion across the water surface to generate lift. By introducing an angle between feet of the user and water surface while moving forward in high speed, the water will "push" the user out of water[48]. The main weakness of this design is the requirement for high speed. The high speed can only be achieved by introducing a powerful motor or similar propulsion device. The propulsion device also needs to be as light as possible.



Raft Shoe

This design utilizes buoyancy to generate upward lift. The raft shoe improves upon the typical patented water walking shoe by making it inflatable, thus easier to transport when needed[49]. The main problem with this design is the large size when used on water. The large size of the raft shoe will introduce difficulty in walking and does not follow the project's design specifications.



APPENDIX E: MATLAB Code for Power Optimization

```
%Program to calculate power requirements/RPM for different  
%hydrofoil configurations
```

```
rho = 1000; %kg/m^3  
%d = .10; %blade width (m)  
t = 0.01; %blade thickness (m)  
Cl = 1.5; %coefficient of lift  
Cd = 0.5; %coefficient of drag  
r1 = .08; %internal radius of foils (m)  
r2 = .14; %external radius of foils (m)  
Fl = 20*9.8; %lift force (N)  
n = 1:1:8; %number of blades  
omega = 1:1:8; %fill with dummy constants to create array  
Fe = Fl./n; %lift per blade
```

```
d = (2*r1*pi/1.5)./n; %space constrained sizing
```

```
%loop for # of blades one through eight  
for j=1:8,
```

```
omega(j) = sqrt(6*Fl/n(j)*1/(rho*d(j)*Cl*(r2^3-r1^3)));
```

```
RPM(j) = omega(j)/(2*pi)*60
```

```
%calculation of drag torque
```

```
Td(j) = n(j)*(1/2*rho*Cd*omega(j)^2*t*1/4*(r2^4-r1^4));
```

```
Power(j) = omega(j)*Td(j);
```

```
end
```

```
%Power = omega*Td; %power in Watts
```

```
HP = 0.00134102209*Power
```

APPENDIX F: Detailed Engineering Drawings

Figure 49: Housing Top

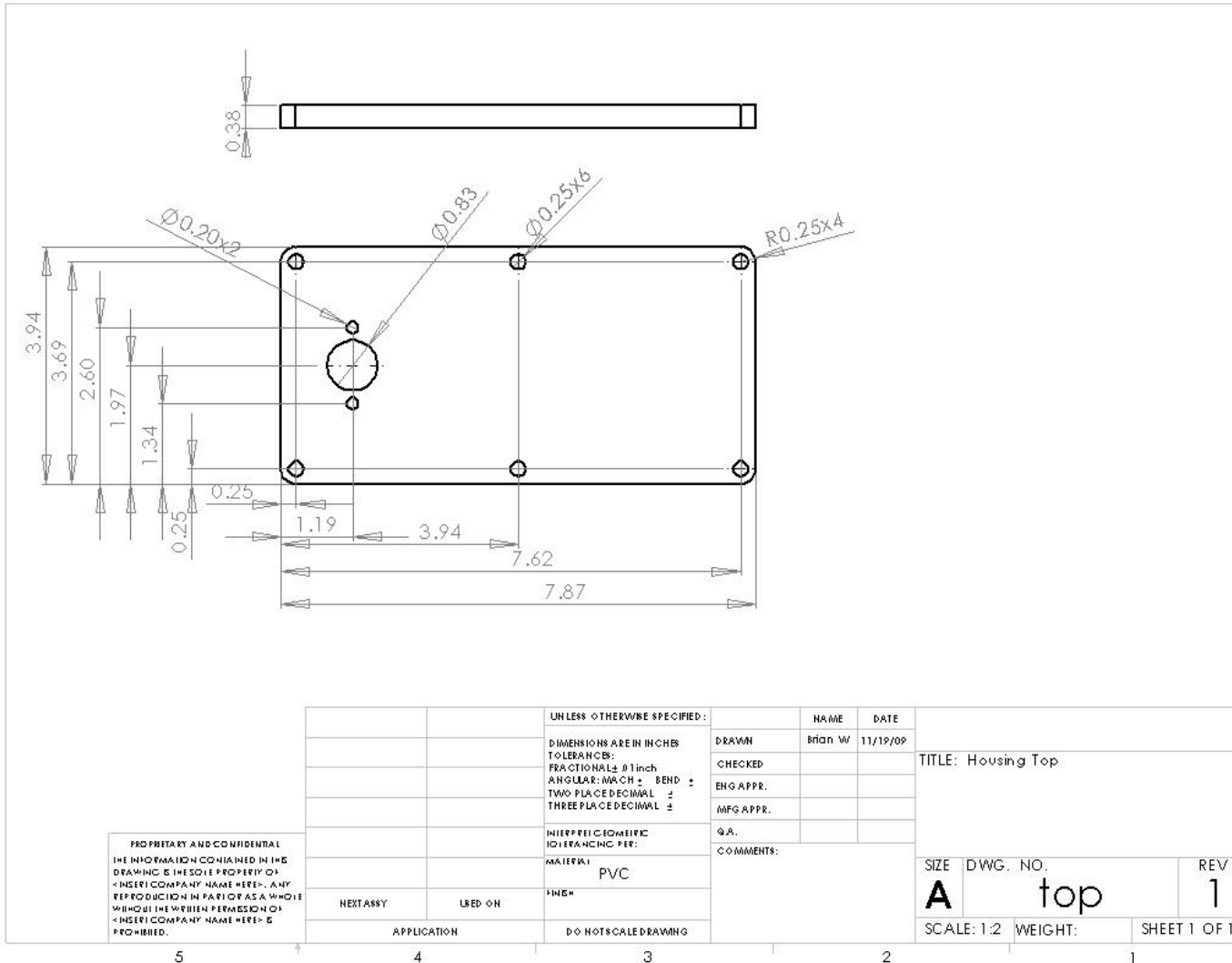
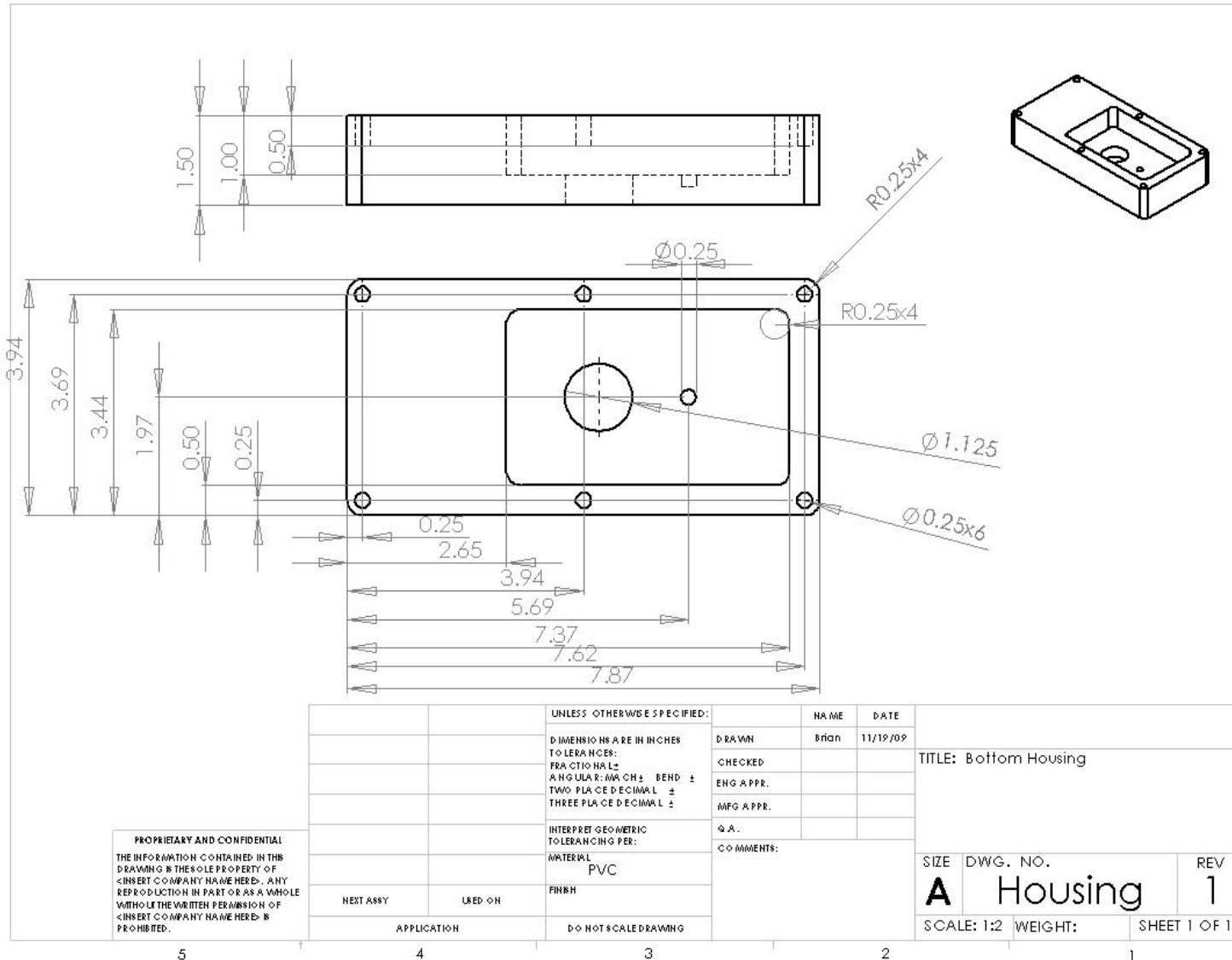


Figure 50: Housing Bottom



PROPRIETARY AND CONFIDENTIAL
 THE INFORMATION CONTAINED IN THIS
 DRAWING IS THE SOLE PROPERTY OF
 <INSERT COMPANY NAME HERE>. ANY
 REPRODUCTION IN PART OR AS A WHOLE
 WITHOUT THE WRITTEN PERMISSION OF
 <INSERT COMPANY NAME HERE> IS
 PROHIBITED.

UNLESS OTHERWISE SPECIFIED:		NAME	DATE		
DIMENSIONS ARE IN INCHES TOLERANCES: FRACTIONAL ± ANGULAR: MATCH ± BEND ± TWO PLACE DECIMAL ± THREE PLACE DECIMAL ±		DRAWN	Brian	11/19/09	TITLE: Bottom Housing
		CHECKED			
		ENG APPR.			
		MFG APPR.			
INTERPRET GEOMETRIC TOLERANCING PER: MATERIAL PVC		Q.A.			SIZE DWG. NO. REV
NEXT ASSY	USED ON	FINISH			A Housing 1
APPLICATION		DO NOT SCALE DRAWING			SCALE: 1:2 WEIGHT: SHEET 1 OF 1

5 4 3 2 1

Figure 51: Hydrofoil Hub

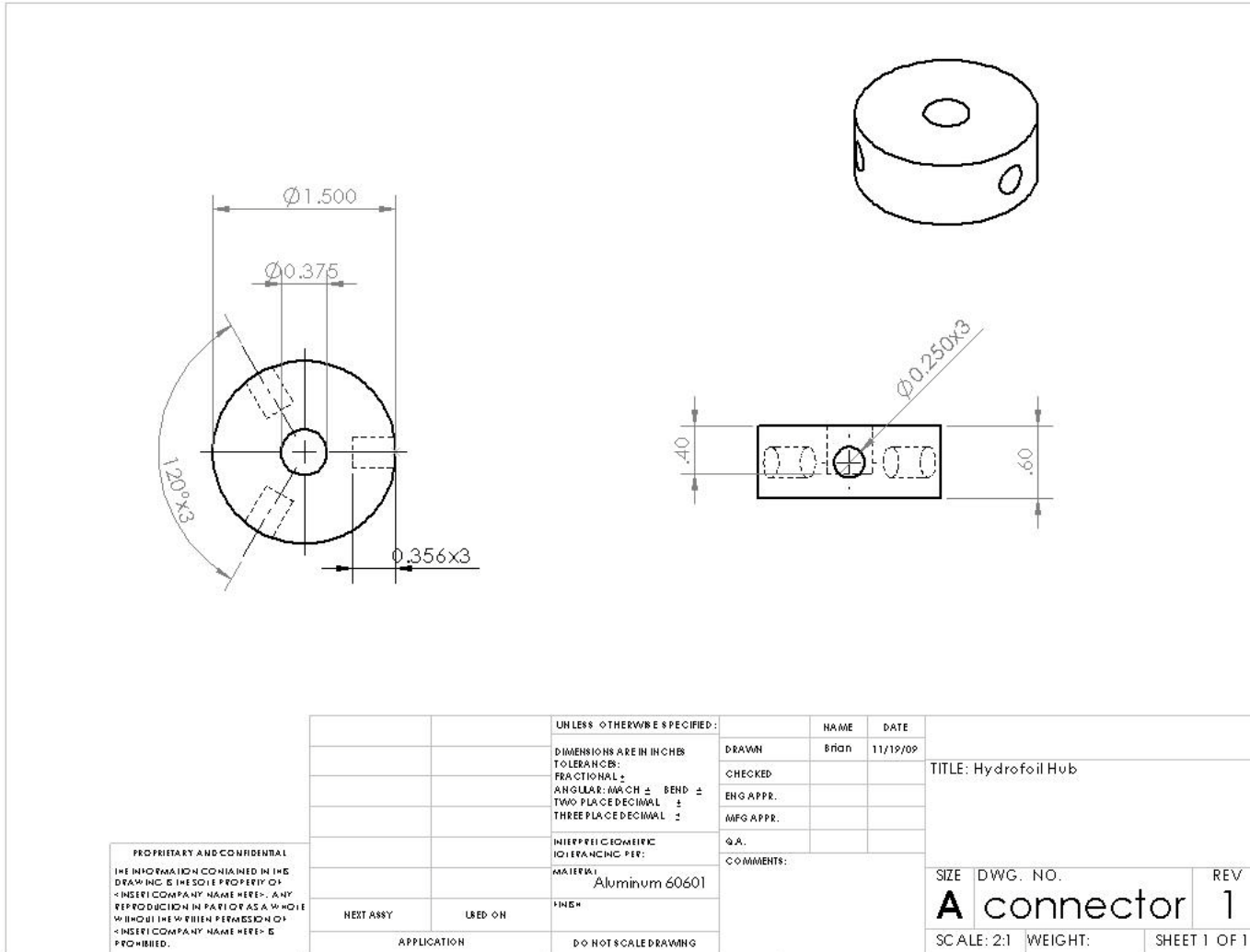
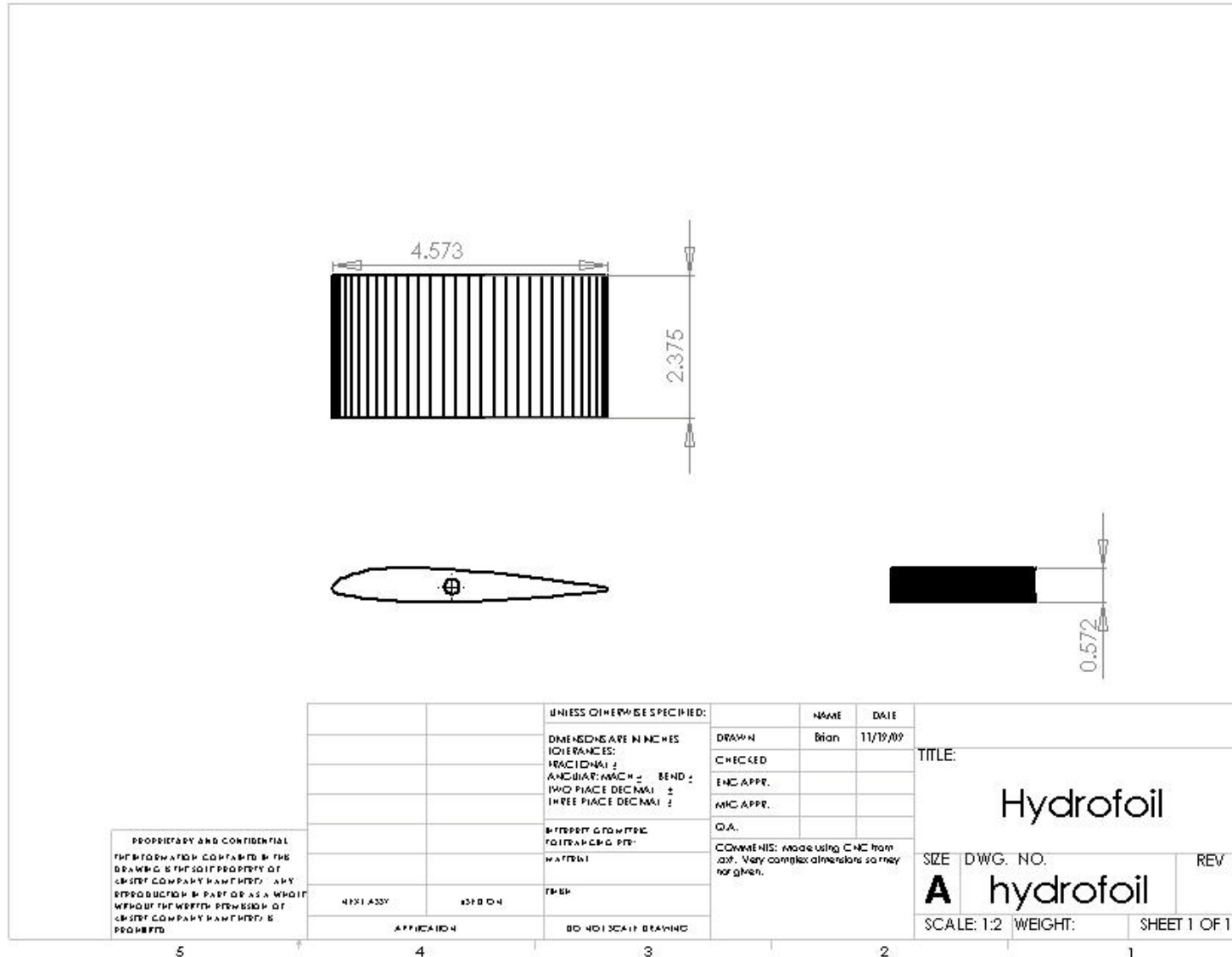


Figure 52: Hydrofoil



-
- [1] Hu, Chan, & Bush, J. (2003). The hydrodynamics of water strider locomotion. *Nature*, 424(6949), 663.
- [2] Bush, J. W. M., & Hu, D. (2006). WALKING ON WATER: Biocomotion at the interface. *Annual Review of Fluid Mechanics*, 38, 339.
- [3] Bush, J., Hu, & Prakash. (2007). The integument of water-walking arthropods: Form and function. *ADVANCES IN INSECT PHYSIOLOGY: INSECT MECHANICS AND CONTROL*, 34, 117.
- [4] Gao, X., & Jiang, L. (2004). Biophysics: Water-repellent legs of water striders. *Nature*, 432(7013), 36.
- [5] Callies, Chen, Marty, Pepin, & Quere. (2005). Microfabricated textured surfaces for super-hydrophobicity investigations. *Microelectronic Engineering*, 78-79, 100.
- [6] Serway, R. A., Moses, C. J., & Moyer, C. A. (1997). *Modern physics*. Fort Worth: Saunders College Pub.
- [7] Sethi, S., & Dhinojwala, A. (2009). Superhydrophobic conductive carbon nanotube coatings for steel. *Langmuir*, 25(8), 4311.
- [8] Keller, J. B. (1998). Surface tension force on a partly submerged body. *Physics of Fluids*, 10(11), 3009.
- [9] Glasheen, & McMahon. (1996). A hydrodynamic model of locomotion in the basilisk lizard. *Nature*, 380(6572), 340.
- [10] Braun, Henry D. Apparatus for Walking upon Water. Patent 4,530,668. July 23, 1985.
- [11] Lieu, Tam T. Water Walking Shoes. Patent 4,801,284. January 31, 1989.
- [12] Thayer, Thomas T. Water Walkers. Patent 5,593,334. January 14, 1997.
- [13] Herbert B. Mason (Editor). *Encyclopaedia of Ships and Shipping*. London. 1908.
- [14] Anderson, John D. (2004), *Introduction to Flight* (5th ed.), McGraw-Hill, pp. 257–261
- [15] Matveev, . (2000). *Estimation and compensation of hydrofoil deformations during operational season*
- [16] Ogden, C., Fryar, C., Carroll, M., & Flegal, K. (2004). Mean body weight, height, and body mass index, united states 1960-2002. *Advance Data from Vital Health Statistics of the National Center for Health Statistics*, (347), 1.
- [17] Gao X, Jiang L (2004). "Biophysics: water-repellent legs of water striders". *Nature* **432** (7013): 36.
- [18] Françoise Brochard-Wyart; David Quéré (2002). *Capillary and Wetting Phenomena — Drops, Bubbles, Pearls, Waves*. Springer.
- [19] Munson, Bruce R. (2008). *Fundamentals of Fluid Mechanics Sixth Edition*. John Wiley & Sons. Hoboken, NJ.
- [20] Miwa, M (2000). "Effects of the surface roughness on sliding angles of water droplets on superhydrophobic surfaces". *Langmuir* **16**: 5754–5760.
- [21] Carroll, Bradley W. 2007. "Archimedes' Principle". Weber State University.
- [22] <http://www.grc.nasa.gov/WWW/K-12/airplane/thrsteq.html>
- [23] "Hydrofoil Basics." 2009. <http://lancet.mit.edu/decavitator/Basics.html>.
- [24] Chatterjee S, Templin RJ. 2007. "Biplane wing planform and flight performance of the feathered dinosaur Microraptor gui". *Proc Natl Acad Sci USA* **104** (5): 1576–80.
- [25] Marzocca, Pier. (2009) "The NACA airfoil series" (PDF). Clarkson University. <http://people.clarkson.edu/~pmarzocc/AE429/The%20NACA%20airfoil%20series.pdf>.
- [26] Stokes (1851). "On the Effect of the Internal Friction of Fluids on the Motion of Pendulums". *Transactions of the Cambridge Philosophical Society* **9**: 8-106.
- [27] http://www.epi-eng.com/piston_engine_technology/power_and_torque.htm
- [28] <http://www.strucalc.com/engineering-resources/normal-stress-bending-stress-shear-stress/>
- [29] http://www.ehow.com/how-does_5591420_happens-water-damage-car_.html
- [30] <http://www.anaheimautomation.com/products/brush/brush-drivers-controllers.php?tid=104>
- [31] <http://www.np.edu.sg/alpha/nbk/alphastu/MotorSelection.html>
- [32] <http://www.pingbattery.com/servlet/the-5/24V-15AH-V2.5-LiFePO4/Detail>
- [33] <http://www.sae.org/technical/papers/810605>
- [34] http://www.centennialofflight.gov/essay/Theories_of_Flight/Skin_Friction/TH11G2.htm
- [35] Lide, D. R., ed. (2005), *CRC Handbook of Chemistry and Physics* (86th ed.), Boca Raton (FL): CRC Press.
- [36] Harris, C. M., and Peirsol, A. G. "Shock and Vibration Handbook", 2001, McGraw Hill.
- [37] Bocquet, L. (2003). The physics of stone skipping. *American Journal of Physics*, 71(2), 150.

-
- [38] Clanet, C., Hersen, F., & Bocquet, L. (2004). Secrets of successful stone-skipping. *Nature*, 427(6969), 29.
- [39] Emsley, John (1998). *The Elements* (3rd ed.). New York: Oxford University Press.
- [40] Peter Atkins (1997). *Physical Chemistry*, 6th edition (W.H. Freeman and Company, New York).
- [41] Aryeh Ben-Na'im *Hydrophobic Interaction* Plenum Press, New York.
- [42] Johnson, C. Scott "Sea Creatures and the Problem of Equipment Damage" *United States Naval Institute Proceedings* August 1978
- [43] Bernardin and Mudawar, "A Cavity Activation and Bubble Growth Model of the Leidenfrost Point," *Transactions of the ASME*, (Vol. 124, Oct. 2002).
- [44] Dand. I. W.: "Hydrodynamic Aspects of Shallow Water Collisions" *Transactions of the Royal Institution of Naval Architects*, Volume 118, 1976.
- [45] Adam, Neil Kensington (1941). *The Physics and Chemistry of Surfaces*, 3rd ed.. Oxford University Press.
- [46] Brown, Theodore L., H. Eugene LeMay, Jr., and Bruce E. Burston. *Chemistry: The Central Science*. 10th ed. Upper Saddle River, NJ: Pearson Education, Inc., 2006.
- [47] McGrail, Sean (2001). *Boats of the World*. Oxford, UK: Oxford University Press.
- [48] "The Physics of Water-skiing." *Welcome to Urbana (OH) City Schools*. Web. 22 Oct. 2009. <<http://www.urbana.k12.oh.us/HSzab/proj200304/michaelkf/KaMichael.htm>>.
- [49] Paulet, Dominique; Presles, Dominique (1999) (in Français). *Architecture navale, connaissance et pratique*. Paris: Éditions de la Villette.